university of groningen

faculty of science and engineering

Incorporation of terpyridine crosslinks in complex coacervate fibers

Kjell Cornelis

February 3, 2022

university of groningen / faculty of science and engineering

University of Groningen

Incorporation of terpyridine crosslinks in complex coacervate fibers

Master's Thesis

To fulfill the requirements for the degree of
Master of Science in Chemistry at University of Groningen
under the supervision of
Prof. dr. M.M.G Kamperman
Dr. G. Monreal Santiago and
J. Sun, MSc

Kjell Cornelis (S4185390)

February 3, 2022

Contents

Acknowledgements

I had a great experience performing my master research project at the Polymer Science group at the Zernike Institute for Advanced Materials. It has been very enriching for my knowledge and skills in research. I would like to thank the people who have helped me during this time.

First, I would like to thank my daily supervisor, Guillermo Monreal Santiago. You gave me a lot of freedom in my research while always making sure that I did not lose my way. Your kindness, support, and humor were never lacking while I was working with you. I wish you the best.

Second, I want to express my gratitude to Marleen Kamperman for receiving me in the Polymer Science group. I always had a lot of joy in our meetings and often ended up with new ideas for the project. Thank you for giving me the opportunity to work in your group. I wish the best for you and the group.

I would also like to thank Jianwu Sun for his kindness and feedback. When Guille could not help me, I could also go to you. Your suggestions were very helpful for my experiments and the interpretation of them. I hope that finishing your PhD will go smoothly.

Lastly, I would like to thank everybody in the Polymer Science group for creating a welcoming and gezellige work environment. Thank you for being open for conversations and giving me advice.

Abstract

The application of complex coacervates is promising in the production of materials. Namely, the physical properties of coacervates can easily be modified by the introduction of salt to the system. Fibers are one of the materials that can be made by complex coacervates. For better application of complex coacervates in this area, a good understanding of their behavior is required. The coacervate fibers can be strengthened by giving the system a fixed orientation so the polymer chains are aligned, which is obtained by stretching of the fibers, but this is often lost by relaxation. This alignment is theorized to be permanent by addition of crosslinks.
To achieve the permanently aligned system, we functionalized the polyelectrolytes, pAA and pDMAP-MAA, with terpyridines, which can form transient crosslinks by complexation with metals. By estimation of the stretchability it was observed that systems where only pAA was terpyrilated were most suited for making fibers. An increase of viscosity and work of adhesion was observed when metals were introduced to the functionalized system. Even though an increase in fiber strength was measured with tensile tests, no increased alignment of the functionalized fibers were observed with Polarized Optical Microscopy or Wide Angle X-ray Scattering after straining the fibers. The mechanism of crosslinking requires further investigation before it can be utilized optimally for fiber spinning.

1 Introduction

The synthesis of polymeric materials often involves the use of organic solvents that are not environmentally friendly. In contrast, polyelectrolytes give the possibility to use water as the solvent. This is made possible by the charges on the polymer backbone that make polyelectrolytes water soluble. On top of this, when mixing solutions of polycations and polyanions in water, complex coacervates are formed due to the charges aggregating by ion-pairing interactions between the oppositely charged units on the polymers [2], as seen in Figure 1. These complexes form a colloidal suspension that is insoluble in water and separates as a polymer rich aqueous phase. This polymer rich phase can then be used for the production of materials. In addition, the complex coacervate can be softened by introducing salt to the system. Namely, the ions from the salt disrupt the electrostatic interactions between the polymers, making the coacervates become more soluble in water [3].

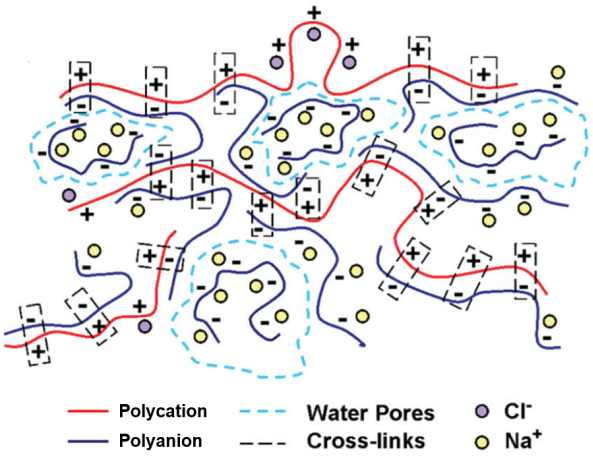

Figure 1: Representation of the complex coacervate structure. Polyelectrolyte chains and their ions are drawn as a solid line. Ion-pairing is shown by the dotted rectangles. Water pores, which contain polyelectrolyte are indicated with dotted blue lines. Adapted from [1]

One of the applications of complex coacervates is as the material for the production of fibers. This can be achieved trough extrusion or pulling of the coacervates. Before these fibers can be used for production, it is interesting to strengthen them by exploring multiple methods. One of the options is to start production with a stiffer material. Using a more rigid polymer leads to less freedom of movement of the polymer chains, thus it could possibly increase the fiber toughness. Another possible path to strengthen the fibers is by having a fixed orientation of the polymers so the chains are aligned. As seen in previous experiments by Sun [4], alignment can be obtained by stretching of the fibers, but this is often lost by relaxation. To make the alignment permanent, transient crosslinks can be incorporated into the system. In such systems the crosslinks enforce orientation by transiently bonding the chains after stretching. These type of crosslinks can already be found in natural materials such as the hydrogen bonds in spider silk and collagen [5, 6]. Where in spider silk, multi-functional crosslinks are found as crystalline β-sheets which improve the elasticity of the silk. And in collagen, glycine creates non-covalent crosslinks with hydrogen bonds that account for the oriented helical conformation of the system. In addition, disulfide bridges in keratin promote a more rigid and stronger network [7].

In terms of crosslinking, previous research by Filippov [8] showed that complex coacervate systems can be crosslinked by metal-ligand binding, increasing its viscosity. The crosslinks are introduced by covalently attaching terpyridine (Tpy) units on the polyelectrolytes. When mixed with divalent metals (M^{2+}), two Tpy units on polymer chains can form a bis complex with one divalent metal, crosslinking the polymers. So, a maximum crosslinking is expected when a ratio of 2:1 Tpy:M^{2+} is used. However, first a mono complex needs to be formed before forming the crosslinking bis complex [9], as seen in the equilibrium in Figure 2.

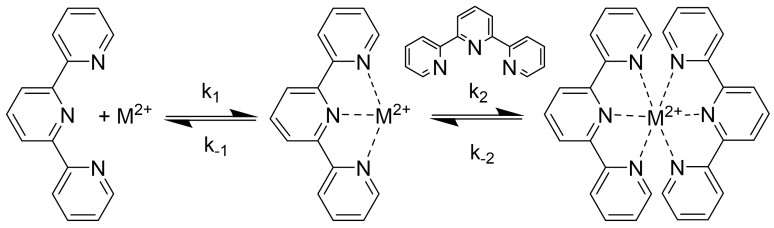

Figure 2: Equilibrium reaction of Tpy ligands with a divalent metal ion to form a mono complex and subsequently a bis complex.

In this master thesis, I attached Tpy ligands to polyelectrolyte systems to incorporate transient crosslinks. By addition of these crosslinks it was expected to form permanent alignment of the polymer chains in the complex coacervates fibers. First, the polycation poly-N-[3-(Dimethylamino)propyl]methacrylamide (pDMAPMAA) was synthesized, while the polyanion polyacrylic acid (pAA) was obtained commercially. These polymers were chosen since pAA was also used in Filippov's work, and pDMAPMAA is very similar to the used positively charged polyelectrolyte. After obtaining the polymers, Tpy ligands were attached on a fraction of units of the polymer backbone. After producing the materials, the optimal salt concentration was determined for the system to create fibers. Then, systems with different metals at varying concentrations were characterized to determine the effect of the terpyridine complexation. The physical properties of the coacervates were characterized by observed stretching and rheological properties. Afterwards, fibers were made with selected coacervates and mechanically characterized using tensile testing. And lastly, alignment in the fibers was determined using Polarized Optical Microscopy (POM) and Wide-Angle X-ray Scattering (WAXS).

2 Material and Methods

2.1 Nomenclature

In this work polyacrylic acid (pAA) is refered to as pA_α and poly(*N*-[3-(Dimethylamino)propyl] methacrylamide) (pDMAPMAA) as pD_α. α represents the molar fraction of Tpy units in the polymer chain. 'NM' indicates an absence of metal.

2.2 Materials

Unless otherwise stated, chemicals were used as received. All chemicals were obtained commercially. Solvents were dried using 3 Å or 4 Å molecular sieves if necessary [10]. All aqueous solutions used water purified by reverse osmosis (R.O. water). Characterization was performed by 1H-NMR in a 400 MHz instrument (appendix A).

2.3 Protonation of low molecular weight polyacrylic acid salt

The Na^+ was removed from NapAA by dissolving 10 g NapAA in a minimal amount of R.O. water. pAA was protonated by adding a solution of 2M HCl untill a pH of 1 was reached. Afterwards the solution was dialyzed against R.O. water with a 1 kDa pore size membrane and subsequently freeze-dried. A white solid was obtained (5.5 g, 55%).

2.4 Synthesis of poly(*N*-[3-(Dimethylamino)propyl]methacrylamide)

The synthesis of pDMAPMAA (Figure 3a) was adapted from literature [11]. DMAPMAA (16 mL, 88 mmol) was dissolved in 120 mL in a round-bottom flask. Potassium persulfate (0.381 g, 1.41 mmol) and Na_2SO_4 (0.083 g, 0.18 mmol) were each dissolved in 40 mL of water. All solutions were separately sparged with N_2 (g) for 4 h. The solutions were mixed together with 50 mL water and stirred for 72 h. The reaction was followed by NMR, and stopped when the spectrum showed a monomer:polymer ratio of 1:1, typically after 72 h. The clear solution was concentrated by freeze-drying. The product was purified first by precipitation from DMF to 50/50 hexane/diethylether mixture and second from water to acetonitrile. After purification, a white solid was obtained (8.3 g, 55%). See Figure 16 for the proton NMR spectrum of the product.

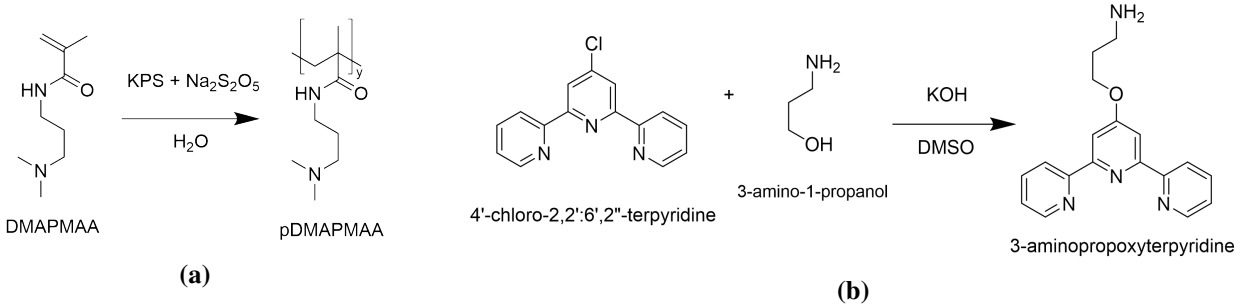

Figure 3: **(a)** Synthesis of pDMAPMAA. **(b)** Synthesis of 3-aminopropoxyterpyridine.

2.5 Synthesis of 3-aminopropoxyterpyridine

The synthesis of 3-aminopropoxyterpyridine in Figure 3b was adapted from literature [8]. Dry DMSO (25 mL) was added to a round-bottom flask. Then 4'-chloro-2,2':6',2''-terpyridine (1.64 g, 6.36 mmol), powdered KOH (1.65 g, 29 mmol), and 3-amino-1-propanol (0.50 mL, 6.7 mmol) were added to the flask under N_2 (g). The mixture was stirred at 60 °C for 30 h. The reaction was stopped by adding the mixture to 300 mL of saturated aqueous K_2CO_3 and subsequently extracted into DCM. The DCM solution was washed once with 0.1 M NaOH and thrice with saturated K_2CO_3. The washed DCM solution was dried with Na_2SO_4 and filtrated. DCM was removed under vacuum by rotary evaporation and subsequently DMSO was removed under high vacuum ($\sim 10^{-2}$ mbar) overnight. The product was obtained as a yellow powder (1.18 g, 3.85 mmol, 60.5%). See Figure 17 for the proton NMR spectrum of the product.

2.6 Synthesis of 4-bromobutoxyterpyridine

The synthesis of 4-bromobutoxyterpyridine in Figure 4a was adapted from literature [8]. 2,6-bis(2-pyridyl)-4(1H)-pyridone (1.00 g, 4.01 mmol) was suspended in 50 mL of dry acetonirile in a round-bottomed flask. Dibromobutane (8.46 g, 39.2 mmol) and K_2CO_3 (1.15 g, 8.07 mmol) were directly added to the white suspension, which was refluxed at 100°C overnight. After cooling, the suspension was filtrated to remove a yellow solid. After concentration using rotary evaporator a brown oil was obtained, which was chromatographed over SiO_2 column using first DCM as eluent and then 5% MeOH in DCM. The 5% MeOH fraction was concentrated in vacuo to obtain 4-bromobutoxyterpyridine as a brown solid (1.219 g, 3.172 mmol, 79.1%). See Figure 18 for the proton NMR spectrum of the product.

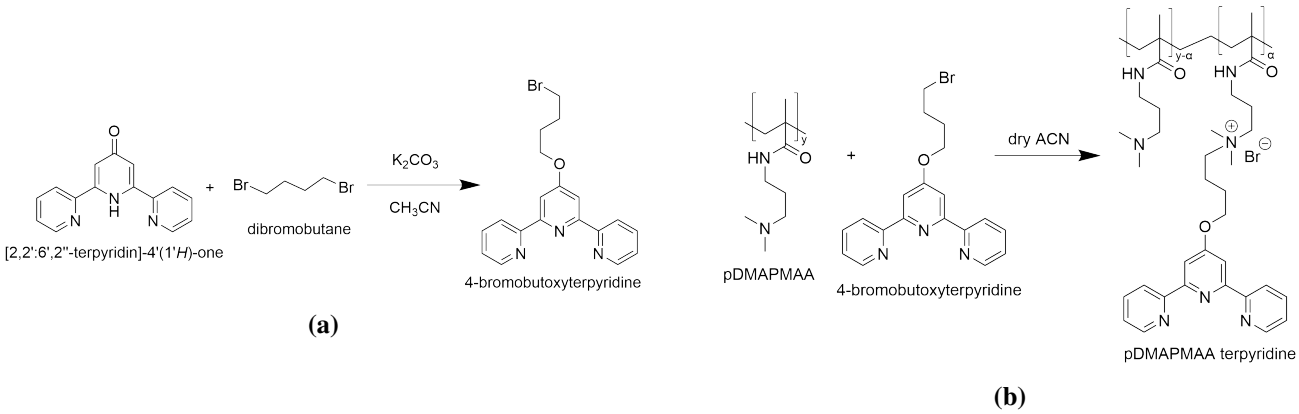

Figure 4: **(a)** Synthesis of 4-bromobutoxyterpyridine. **(b)** Synthesis of pDMAPMAA terpyridine.

2.7 Terpyridylation of poly(*N*-[3-(Dimethylamino)propyl]methacrylamide)

The terpyridylation of pDMAPMAA with a grafting percentage of 5% in Figure 4b was adapted from literature [8]. pDMAPMAA (1.7 g, 10 mmol) was added to a round-bottomed flask. Dry acetonitrile (60 mL) was added to the flask followed by addition of 3-terpyridyloxy bromopropane (0.20 g, 0.5 mmol). The mixture was stirred for 3 days at 55°C. The reaction was stopped and the mixture was concentrated under vacuum by rotary evaporation. The product was purified by precipitation from a minimal amount of acetonitrile solution to a 1:1 diethyl ether and hexane mixture. After drying in a

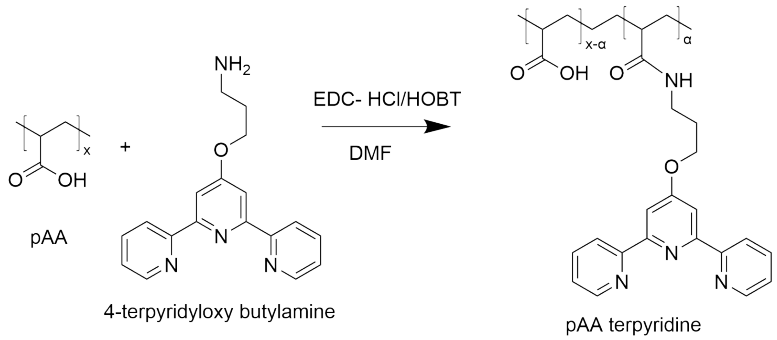

Figure 5: synthesis of pAA terpyridine.

vacuum oven the product (1.038 g, 56.0%) was obtained as an orange solid. A functionalization of 3.8% Tpy units was found using proton NMR analysis. See Figure 19 for the proton NMR spectrum of the product.

2.8 Terpyridylation of poly(acrylic acid)

The synthesis of 5% Tpy grafted pAA in Figure 5 was adapted from literature [8]. pAA (1.24 g, 17.2 mmol units) was dissolved in 60 mL dry DMF and bubbled with N_2 for 1 h. EDC (0.1804 g, 0.946 mmol) and HOBT (0.1276 g, 0.946 mmol) were both dissolved in minimal DMF (10 mL for EDC and 3 mL for HOBT). After 30 min of sparging with N_2, the solution of EDC and HOBT were injected into the pAA solution. After 50 min of stirring a suspension of 3-aminopropoxyterpyridine (0.264 g, 0.86 mmol) in minimal DMF (5 mL) was added. After 16 h of stirring the mixture was transferred to a 1 kDa dialysis membrane. After 4 days of dialysis against R.O. water, controlled by UV-vis, the content of the dialysis bag became turbid with a pink precipitate. To ensure solubility, only the dissolved content was freeze-dried. pAA with terpyridylation of a range of 1.7% to 2.5% was obtained as a pink powder. See Figure 20 for the proton NMR spectrum of the product.

2.9 Preparation of coacervates

Polyelectrolyte solutions were prepared in concentrations of 0.1 M in monomer units in R.O. water. When making the solution the pH was adjusted to 7 using NaOH and HCl 2M solutions to ensure the polymers were in their charged forms. Pure NaCl was added to both solutions before mixing the polyelectrolytes. In the samples where metal was added, the metal was included as a MCl_2 salt. The MCl_2 was added from a 0.1 M stock solution to the polyelectrolyte solution without Tpy groups. The polyelectrolytes solutions were mixed and allowed to equilibrate. After centrifugation at 4500 RCF for 20 min, the supernatant was decanted to obtain concentrated complex coacervates.

2.10 Indication of stretchability

A qualitative indication of the fiber strength was obtained by stretching a small amount of coacervate (0.2 mL) between two spatulas until the coacervate teared apart. The length at break was then measured as result. A longer length before breaking of the coacervate indicates that the coacervate would make stronger fibers.

2.11 Rheology

Frequency sweep and viscosity versus shear rate measurements were performed on a MCR300 (Anton Paar) with a CP25-1 mm cone plate (D: 25 mm; Angle: 1°). The samples were prepared by placing 0.3 mL of coacervate on the bottom metal plate. Then the gap was set to the trimming position and excess coacervate was removed. The dilute phase was poured on the geometry to prevent drying of the coacervate. Viscosity was determined at shear rates (γ) of 0.1-100 Hz. Frequency sweeps were measured from 0.1 to 100 rad/s within the linear viscoelastic regime at a constant strain of 1%.
For tack tests, a MCR302e (Anton Paar) was used with a sand blasted parallel plate (PP10/S D: 10 mm). 0.2 ml of sample was loaded onto the geometry. The plate was set to a gap size of 0.05 mm and left to rest for 2 minutes, afterwards the plate lifts up with a speed of 500 µm/s.

2.12 Making fibers

Fibers were prepared by transferring 0.5 mL of complex coacervate into a syringe. The syringe was centrifuged at 2000 rpm for 20 minutes to remove air bubbles. Using a programmable syringe pump, AL-4000, fibers were pumped out with a constant flow, vertically into a coagulation bath containing water or ethanol. The flow depends on the viscosity of the used coacervate. Syringe needles were used with an inner diameter of 0.5 mm. See Figure 11 for the setup. The collected fibers were dried in air for different time lengths.

2.13 Tensile testing

The mechanical properties of the fibers were characterized using a 100N tensile tester Instron electromechanical load frame. The cross section area of the samples were determined by assuming a rectangular geometry. The crosshead was displaced upwards with 10 mm/min, starting from a gap size of 1 cm.

2.14 Polarized Optical Microscopy (POM)

The alignment of the fibers was characterized using the polarised light method on a Nikon Eclipse 600 Optical Microscope with a NCB 11 filter. Samples were loaded and observed using the 10x objective.

2.15 Wide-Angle X-ray Scattering (WAXS)

WAXS experiments were performed using a wavelength of 1.54840 Å with an acquisition time of 300 s. The measurements were recorded with a single fiber prepared by extruding a small amount of coacervate, with a sample-to-detector distance of 70 mm.

3 Results and Discussion

3.1 Material preparation

pAA and pDMAPMAA were chosen as the model for polyelectrolytes the complex coacervates. To study the effect of Tpy crosslinks on this system, the polyelectrolytes were terpyridylated based on the synthesis in literature [8].
Tpy was attached to the pAA with a functionalization of 5% using the reaction described in Figure 5. In the first synthesis experiments pAA was used with a molecular weight of $\sim$ 450.000 g/mol. Unfortunately, the pAA had a poor solubility in water after terpyridylation with a content of 5% Tpy units. To increase the solubility, a functionalization of only 2.5% Tpy was used. Unfortunately this still yielded in a poor solubility of pAA in water. Therefore, a lower molecular weight ($\sim$ 5.000 g/mol) variant of pAA was used. This however could only be purchased as a pAA sodium salt. The pAA being in the salt form could lead to a poor solubility in DMF, the solvent used for the terpyridylation. To remove the Na^+ ion, the purchased NapAA was protonated and dialyzed by the method described before.
For the 5% terpyridylation of pAA a pink solid was observed to crash out during dialysis. The pink solid was collected separately from the turbid white liquid content of the dialysis bag. Interestingly, the product obtained from the pink solid showed a higher grafting percentage on proton NMR in Figure 21 than the product from the liquid content in Figure 20 (4.1% Tpy units instead of 2.3%). The pink solid did not dissolve in water at 0.1 M, even after neutralizing the pH. Fortunately, the product obtained from the liquid content did dissolve in water and was therefore used for the preparation of the complex coacervates.
pDMAPMAA was terpyridylated using the reaction described in Figure 4b. When aiming for a functionalization of 5% Tpy units, an actual functionalization of 3.8 % was found using proton NMR analysis in Figure 19.

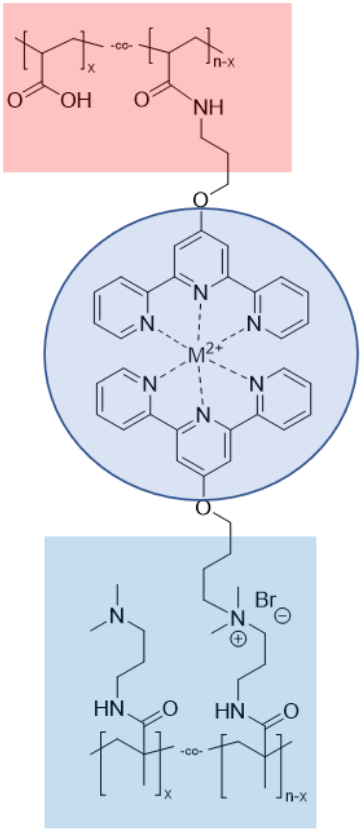

Figure 6: Visualisation of the complex coacervates consisting of polyelectrolytes pAA (pA) in red and pDMAPMAA (pD) in blue with Tpy units. Metal ions (M^{2+}) form bis complexes with Tpy to create transient crosslinks.

Characterization data for the synthesises can be found in appendix A. Different combinations of complexes were made: complexes without modification of the polyelectrolytes (pA/pD), complexes with only one terpyridylated polyelectrolyte ($pA_{0.05}$/pD or pA/$pD_{0.05}$), and complexes with both polyelectrolytes terpyridylated ($pA_{0.05}$/$pD_{0.05}$). Figure 6 portrays the polymers when crosslinked.

3.2 Coacervate stretchability

First, a series of complexes without modifications (pA/pD) were made with a decreasing salt concentration, see Table 1. The maximum stretching lengths of the complexes were determined as previously described, for a demonstration see Figure 7a. The complex with 0.5 M NaCl did not stretch at all since it was a liquid. Then the complex with 0.25 M NaCl stretched to a maximum of 0.5 cm. As

Table 1: The maximum stretching performed as in Figure 7a for complex coacervates without additional crosslinks (pA/pD) at different salt concentrations.

complex	[NaCl]	length maximum stretching
pA/pD	0.5 M	0 cm (liquid)
	0.25 M	0.5 cm
	0.2 M	1.5 cm
	0.1 M	15 cm
	0.05 M	30 cm
	0 M	0 cm (precipitate)

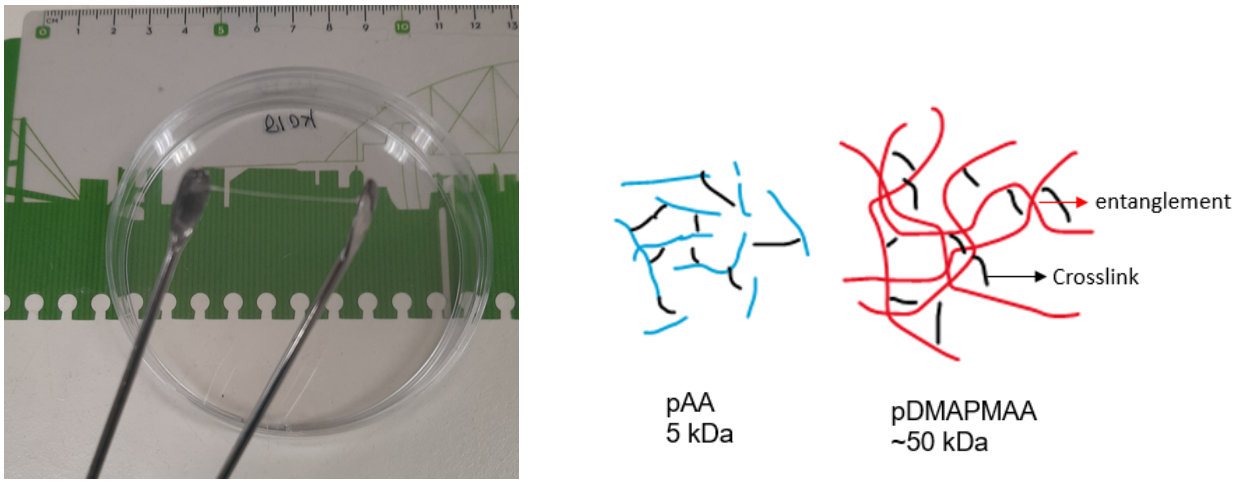

(a) **(b)**

Figure 7: **(a)** Demonstration of stretching of pA/pD complex at 0.05 M NaCl. **(b)** Visualisation of crosslinks in pA units and crosslinks in pD units. Since pD has a larger Mw it is expected to cause more entanglements in the polymer configuration, leading to a higher hardening effect of crosslinking.

expected, the maximum stretching length increased when decreasing the salt concentration. And ultimately, when not adding any salt to the solutions resulted the coacervate to precipitate. The complex with 0.05 M salt yielded the largest maximum stretching, thus this salt concentration was used when preparing further coacervates.

Next, the effect of Tpy crosslinks on the maximum stretching of coacervates was determined with modified pDMAPMAA (Table 2). pA/pD$_{0.05}$-Zn^{2+} was prepared at 0.05 M NaCl with a Tpy:M^{2+} ratio of 2:1, which resulted in a brittle gel. To soften the complex, the salt concentration was increased to 0.5 M, but the complex still resulted in a gel, contrary to the softening effect salt has on coacervates. To make the coacervate even more liquid, crosslinking was reduced by preparing pA/pD$_{0.025}$-Zn^{2+} and the concentration of Zn^{2+} was decreased accordingly to reach a 2:1 ratio of Tpy:Zn^{2+}, see Table 3. However pA/pD$_{0.025}$-Zn^{2+} still resulted in a brittle gel. Thus, a series of complexes with decreasing concentrations of Zn^{2+} was prepared. It is important to note that when decreasing the concentration of the metal, the ratio of Tpy:M_{2+} increases and the degree of crosslinking decreases, as is explained by the equilibrium in Figure 2. Unfortunately, only at very low concentrations of Zn^{2+} the pA/pD$_{0.025}$-Zn^{2+} complex coacervates show stretching of only 4 cm, compared to the 30 cm obtained by the

Table 2: Stretching of complex coacervates with additional crosslinks on pD using Zn^{2+} ($pA/pD_{0.05}$-Zn^{2+}) at a 2:1 Tpy:M^{2+} ratio. The NaCl concentration is increased to soften the material, since the coacervate showed no stretching at 0.05 M NaCl.

complex	[NaCl]	M^{2+} units mol%	Tpy:M^{2+} ratio	maximum stretching
$pA/pD_{0.05}$-Zn^{2+}	0.05 M	0.025%	2:1	0 cm (brittle gel)
	0.1 M	0.025%	2:1	0 cm (brittle gel)
	0.15 M	0.025%	2:1	0 cm (brittle gel)
	0.2 M	0.025%	2:1	0 cm (brittle gel)
	0.5 M	0.025%	2:1	0 cm (brittle gel)

Table 3: Stretching of complex coacervates with additional crosslinks on pD using Zn^{2+} ($pA/pD_{0.05}$-Zn^{2+}). The mol% of Zn^{2+} is decreased to reduce the amount of crosslinks. The concentration of NaCl is also increased to soften the complex.

complex	[NaCl]	M^{2+} units mol%	Tpy:M^{2+}	maximum stretching
$pA/pD_{0.025}$-Zn^{2+}	0.05 M	1.25%	2:1	0 cm (brittle gel)
	0.05 M	0.625%	2:0.5	0 cm (brittle gel)
	0.05 M	0.313%	2:0.25	0 cm (brittle gel)
	0.05 M	0.156%	2:0.125	0 cm (brittle gel)
	0.05 M	0.0782%	2:0.0625	0 cm (gel)
	0.1 M	0.156%	2:0.125	0 cm (gel)
	0.1 M	0.0313%	2:0.025	4 cm stretching
	0.1 M	0.0156%	2:0.0125	4 cm stretching
	0.5 M	0.313%	2:0.25	0 cm (brittle gel)
	0.5 M	0.156%	2:0.125	5 cm

non-modified pA/pD system.

According to Filippov [8], Mn^{2+} has a lower binding affinity compared to Zn^{2+}, thus leading to a softer material when used in the coacervate systems with Tpy. Coacervates of $pA/pD_{0.025}$-Mn^{2+} were prepared as Table 4. The prepared coacervates with Mn^{2+} showed good stretching, thus can be used to make fibers.
Coacervates with Tpy on the polyanion were also prepared ($pA_{0.05}$/pD). Interestingly, these coacervates showed a large increase in maximum stretching when fully crosslinking with Mn^{2+}, Zn^{2+}, and Co^{2+}. This shows that introducing Tpy crosslinks to coacervates can enhance the maximum stretching, and could possibly increase the fiber strength.

When adding metal above the 2:1 ratio of Tpy:M^{2+} the degree of crosslinking is expected to decrease since the equilibrium of Tpy (Figure 2) is pushed back into the mono substituted complex [12]. $pA_{0.05}$/pD samples were prepared with a 2:2 ratio Tpy:M^{2+} to test this effect of 'oversaturation' (Table 5). Interestingly, oversaturated $pA_{0.05}$/pD-Zn^{2+} yields a larger maximum stretching than the

Table 4: Stretching of complex coacervates with additional crosslinks using Zn^{2+}, Mn^{2+}, or Co^{2+}. Coacervates were prepared with Tpy on pA($pA_{0.05}$/pD) or with Tpy on pD (pA/$pD_{0.025}$).

complex	[NaCl]	M^{2+} units mol%	Tpy:M^{2+}	maximum stretching
pA/$pD_{0.025}$-Mn^{2+}	0.05 M	0.156%	2:0.125	30 cm
	0.05 M	0.0782 %	2:0.0625	40 cm
$pA_{0.05}$/pD-Mn^{2+}	0.05 M	0%	2:0	15 cm
	0.05 M	0.156%	2:0.25	18 cm
	0.05 M	2.5%	2:1	60 cm
$pA_{0.05}$/pD-Zn^{2+}	0.05 M	2.5%	2:1	60 cm
$pA_{0.05}$/pD-Co^{2+}	0.05 M	2.5%	2:1	70 cm

Table 5: Stretching of complex coacervates with crosslinks at an 'oversaturated' 2:2 Tpy:M^{2+} ratio, pushing back the Tpy equilibrium to the mono complex.

complex	[NaCl]	M^{2+} units mol%	Tpy:M^{2+}	maximum stretching
$pA_{0.05}$/pD-Mn^{2+}	0.05 M	5%	2:2	60 cm
$pA_{0.05}$/pD-Zn^{2+}	0.05 M	5%	2:2	100 cm
$pA_{0.05}$/pD-Co^{2+}	0.05 M	5%	2:2	60 cm

2:1 ratio, even though it is expected have a reduced crosslinking. However, $pA_{0.05}$/pD-Mn^{2+}, and $pA_{0.05}$/pD-Co^{2+} with a 2:2 ratio show a similar maximum stretching with the 2:1 Tpy:M^{2+} ratio. $pA_{0.05}$/pD and pA/$pD_{0.05}$ were compared for 'oversaturation', see Table 6. The samples of $pA_{0.05}$/pD had good stretching, while for pA/$pD_{0.05}$ the material could not be stretched since no coacervate was formed or the system precipitated. This shows a very clear difference when crosslinking pA versus crosslinking pD. Namely, crosslinking pD has a much larger effect, leading to more solid properties. This can be explained by the larger molecular weight of pD compared to pA. Since the chains are longer for pD, entanglements are more likely to occur when the system is crosslinked, as is visualised in Figure 7b.

Table 6: Stretching of complex coacervates comparing crosslinks on pA ($pA_{0.05}$/pD) with crosslinks on pD (pA/$pD_{0.05}$) using Zn^{2+}, Mn^{2+}, or Co^{2+} at an 'oversaturated' ratio of Tpy:M^{2+}.

complex	[NaCl]	M^{2+} units mol%	Tpy:M^{2+}	maximum stretching
$pA_{0.05}$/pD-Zn^{2+}	0.05 M	5%	2:2	100 cm
$pA_{0.05}$/pD-Mn^{2+}	0.05 M	5%	2:2	60 cm
$pA_{0.05}$/pD-Co^{2+}	0.05 M	5%	2:2	60 cm
pA/$pD_{0.05}$-Zn^{2+}	0.05 M	5%	2:2	0 cm (no coacervate)
pA/$pD_{0.05}$-Mn^{2+}	0.05 M	5%	2:2	0 cm (no coacervate)
pA/$pD_{0.05}$-Co^{2+}	0.05 M	5%	2:2	0 cm (precipitate)

Table 7: Stretching of complex coacervates with Tpy on both polyelectrolytes ($pA_{0.05}/pD_{0.05}$), allowing crosslinking between the polyelectrolytes.

complex	[NaCl]	M^{2+} units mol%	Tpy:M^{2+}	maximum stretching
$pA_{0.05}/pD_{0.05}$-Mn^{2+}	0.05	2.5%	2:0.5	0 cm (gel)
	0.05	5%	2:1	0 cm (gel)
$pA_{0.05}/pD_{0.05}$-Zn^{2+}	0.05	10%	2:2	0 cm (no coacervate)

Tpy on both polyelectrolytes allows for crosslinking between the two species. The effect of this was studied with the $pA_{0.05}/pD_{0.05}$ system as seen in Table 7. Unfortunately, $pA_{0.05}/pD_{0.05}$-Mn^{2+} created a gel that could not be stretched, and $pA_{0.05}/pD_{0.05}$-Zn^{2+} did not create a coacervate at all.
Based on the results of the stretchability, the coacervates with terpyridylated pA were the most suited for making fibers, since they gave the longest maximum stretching. The $pA_{0.05}$/pD system was therefore used with a NaCl concentration of 0.05 M as the basis for rheological experiments and producing fibers.

3.3 Rheology

Frequency sweeps were recorded to demonstrate the change in viscoelastic behaviour of the complex coacervates. Upon performing the frequency sweeps the storage modulus G' and loss modulus G" were obtained. The G' describes the elastic part of the viscoelastic behaviour and G" describes the viscous part. If G' of a sample is higher than the G", the sample is described to be more solid-like. While when G" of sample is greater than G', the sample is more in a liquid state. As stated before, all complexes were prepared with a NaCl concentration of 0.05 M.
First a strain sweep was performed on pA/pD to ensure we are measuring in the linear viscoelastic region. The strain sweep in the appendix Figure 22 shows that the viscoelastic response stays linear even at a strain of 10%. So, the frequency sweeps were measured at a constant strain of 1%, since this is well inside the linear viscoelastic region.

The first observed trend is that for all the measured frequency sweeps in Figure 8 and 9, G" is greater than G'. This indicates that all prepared complex coacervates have a more liquid-like behavior.
To characterize the influence of introducing Tpy units in the complex coacervates, frequency sweeps were compared for pA/pD, $pA_{0.025}$/pD, and $pA_{0.05}$/pD without the addition of M^{2+}. Functionalized pD was not analyzed since it was found out that pA was more suitable for producing fibers. In Figure 8a $pA_{0.025}$/pD and $pA_{0.05}$/pD show an increased G' and G" from pA/pD, while $pA_{0.05}$/pD shows the largest increase. Based on this, incorporating Tpy to pA without metal crosslinks seems to already increase both moduli.

When adding metal ions to the complex coacervates with Tpy, $pA_{0.025}$/pD-M^{2+} and $pA_{0.05}$/pD-M^{2+} both show the same trend: Mn^{2+} increases both moduli, while Zn^{2+} increases them even more. This trend agrees with the order of binding affinities found by Filippov [8]. However, $pA_{0.05}$/pD-Co^{2+} shows a very little increase from $pA_{0.05}$/pD-NM, while $pA_{0.025}$/pD-Co^{2+} has the same response without metal. This does not agree with the trend found in literature, where Co^{2+} has an even higher binding affinity than Zn^{2+}. Thus, a higher binding affinity does necessarily lead to and increase in the moduli. This could be because after the strong Co^{2+} crosslinks are broken, it takes a long time

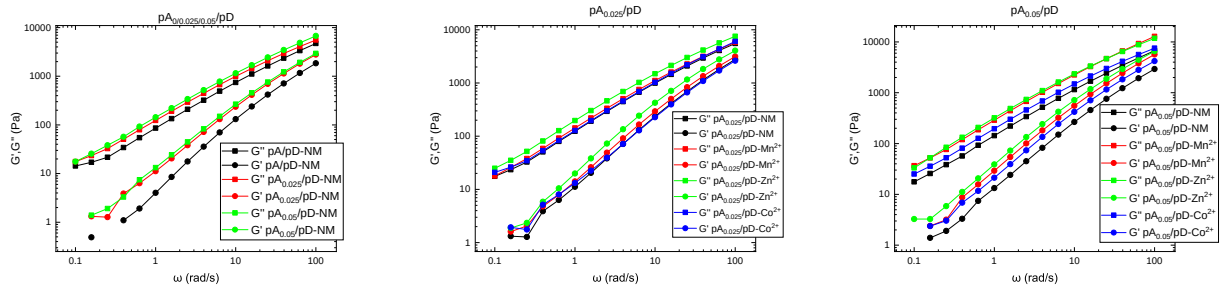

(a) **(b)** **(c)**

Figure 8: **(a)** Frequency dependent storage (G') and loss (G") moduli of pA/pD, $pA_{0.025}$/pD, and $pA_{0.05}$/pD. **(b)** Frequency dependent storage (G') and loss (G") moduli of $pA_{0.025}$/pD-M^{2+}. **(c)** Frequency dependent storage (G') and loss (G") moduli of $pA_{0.05}$/pD-M^{2+}.

to reform those crosslinks. If $pA_{0.05}$/pD-Co^{2+} was recorded with a longer timescale, the terpyridine could have enough time to form new bonds and demonstrate the effects of its high binding affinity. As expected, the $pA_{0.05}$/pD-M^{2+} systems show a larger increase in moduli than the corresponding $pA_{0.025}$/pD-M^{2+} since there is more crosslinking.

A mixture of divalent metals was also employed to observe if the properties can be fine-tuned by mixing a strong (Zn^{2+}) and weak (Mn^{2+}) crosslinking metal. The $pA_{0.05}$/pD-Zn^{2+}/Mn^{2+} coacervate with mixed metals was prepared so that there was a 4:1 Tpy:Zn^{2+} ratio and a 4:1 Tpy:Mn^{2+} ratio. This was compared to a reference $pA_{0.05}$/pD-Zn^{2+} coacervate with a 4:1 Tpy:Zn^{2+} ratio. Both coacervates have the same amount of Zn^{2+} crosslinks, but the $pA_{0.05}$/pD-Zn^{2+}/Mn^{2+} has additional crosslinks from Mn^{2+} bonds. In theory the mixed $pA_{0.05}$/pD-Zn^{2+}/Mn^{2+} should yield a higher G' and G" than the reference $pA_{0.05}$/pD-Zn^{2+}, since it has additional crosslinks. Interestingly, the $pA_{0.05}$/pD-Zn^{2+}/Mn^{2+} coacervate and the reference have the same response in the recorded frequency sweep of Figure 9a. This can be explained by the large difference in crosslink strength between the metals. The effect of Zn^{2+} crosslinks is so strong that the weak effect of the Mn^{2+} crosslinks can not be observed.

To characterize the previously discussed effect of 'oversaturation', the frequency sweeps in Figure 9b and 9c were recorded. Contrary to the stretching results, the plots show no significant difference when excess metal is added above the 1:2 Tpy:Zn^{2+} ratio. This suggests that the bis complex in Figure 2 that is responsible of crosslinking, remains dominant when additional M^{2+} ions are introduced. The stretching test seems to more sensitive for changes in phyiscal properties.

Tack tests were also recorded to quantify the coacervate stretchability that was estimated before, see Table 8. At a lift speed of 100 µm/s, only Mn^{2+} showed a increased work of adhesion measured for $pA_{0.025}$/pD-M^{2+} (Figure 10a). However, at a lift speed of 500 µm/s $pA_{0.025}$/pD-Zn^{2+} also showed a increased work of adhesion, but still lower than Mn^{2+}, see Figure 10b. This is not the same trend that was seen for the frequency sweeps, where the order for the storage and loss moduli were Zn^{2+}>Mn^{2+}>NM. For the $pA_{0.05}$/pD-M^{2+} system, the expected trend from the frequency sweeps is seen back in the tack test at 500 µm/s in Figure 10c. Namely, $pA_{0.05}$/pD-Zn^{2+} has a greater work of adhesion than Mn^{2+}, which in turn is greater than when no metal is added. The $pA_{0.05}$/pD-Co^{2+} system was also measured, which had the same work as the NM, this fits in the trend that was found for the frequency sweeps.

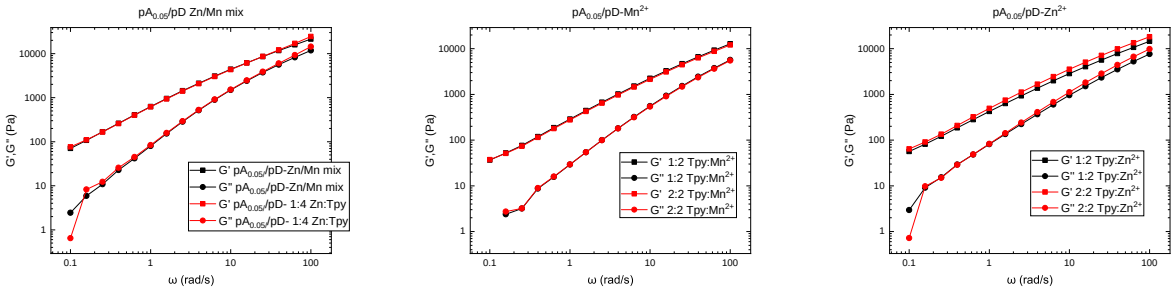

(a) **(b)** **(c)**

Figure 9: **(a)** Frequency dependent storage (G') and loss (G") moduli of $pA_{0.05}$/pD with mixed metals. **(b)** Frequency dependent storage (G') and loss (G") moduli of $pA_{0.05}$/pD-Mn^{2+} at 1:2 and 2:2 Tpy:Mn^{2+} ratio. **(c)** Frequency dependent storage (G') and loss (G") moduli of $pA_{0.05}$/pD-Zn^{2+}.at 1:2 and 2:2 Tpy:Zn^{2+} ratio.

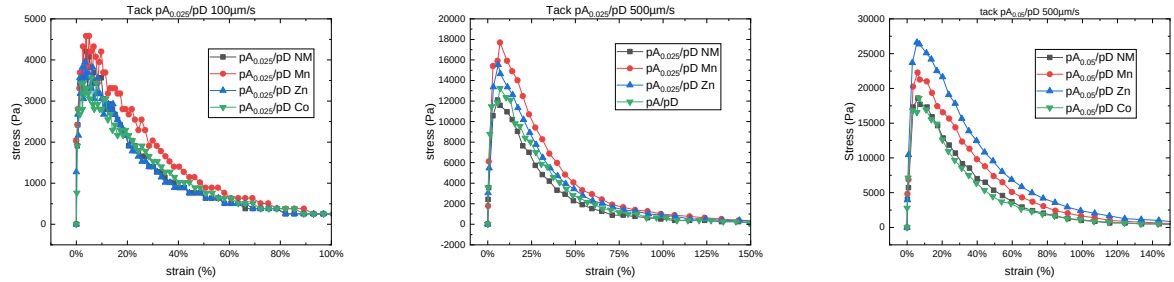

(a) **(b)** **(c)**

Figure 10: Tack tests of **(a)** $pA_{0.025}$/pD-M^{2+} with lift speed of 100 µm/s, **(b)** pA/pD and $pA_{0.025}$/pD-M^{2+} with lift speed of 500 µm/s, and **(c)** $pA_{0.05}$/pD-M^{2+} with lift speed 500 µm/s

3.4 Producing fibers

Fibers of the unmodified pA/pD complexes were prepared from coacervates at a NaCl concentration of 0.05 M. This was done by first filling a syringe with 3 mL coacervate and placing it in a syringe pump that was set up vertically in direct contact to a coagulation bath as seen in Figure 11. The coagulation bath was filled with R.O. water. When the complex enters the coagulation bath the salt concentration decreases substantially. This is done since removing the NaCl counterions should make the complex more solid, and thus making the fibers stronger. Unfortunately, coagulation in R.O. water with pA/pD resulted in very soft, liquid like fibers. Thus, the complex does not gain solid-like properties when the NaCl ions are removed from the system.

Fortunately ethanol can help with the coagulation, because complex coacervates do not dissolve in ethanol. Thus when the complex coavervate is injected into ethanol, the complex precipitates. First a 50:50 mixture of ethanol and water was used as coagulation bath, but this still resulted in fibers that were too weak. Fortunately, using only ethanol as bath resulted in solid fibers that could easily be collected. From this point onward all fibers were prepared by coagulation in ethanol. After collection the fibers were left to dry in air overnight. The moisture content of fibers immediately after production was measured to be around 40%. Overnight this decreased to 20%. After 1 week the moisture content was still in the range of 20%.

An interesting trend seen from the fiber production was that fibers prepared with $pA_{0.05}$/pD-M^{2+} have

Table 8: Tack tests results.

system	M^{2+}	lift speed (µm/s)	Work of adhesion (J/m^2)	max stress (Pa)
$pA_{0.025}$/pD	-	100	0.61	4200
	Mn^{2+}		0.81	4580
	Zn^{2+}		0.60	3950
	Co^{2+}		0.61	3570
pA/pD	-	500	2.40	13200
$pA_{0.025}$/pD	-		2.06	12100
	Mn^{2+}		3.36	17700
	Zn^{2+}		2.77	15500
$pA_{0.05}$/pD	-	500	3.78	18600
	Mn^{2+}		4.95	22300
	Zn^{2+}		6.41	26600
	Co^{2+}		3.58	18600

Table 9: cross section of producedfibers

$pA_{0.05}$/pD-M^{2+}	no metal	Zn^{2+}	Mn^{2+}
average cross section area (mm^2)	0.18	0.34	0.22

a much larger cross section area when metals are added than fibers without metal, see Table 9 for details. This is explained by the increased viscosity of the crosslinked complexes. A lower viscosity causes a faster flow of the syringe, thinning the fiber. This effect is even more enhanced by the vertical setup required for producing fibers, since the low viscosity coacervates are pulled out of the syringe by gravity.

3.5 Tensile testing

A large amount of coacervate material is needed to produce fibers for analysis. Thus the parameters for analysis were carefully chosen. Based on the results of maximum stretching and rheology data the following complexes were used for fibers: pA/pD, $pA_{0.05}$/pD-Zn^{2+}, and $pA_{0.05}$/pD-Mn^{2+}.

3.5.1 Dry fibers

The stretchability tests indicated that $pA_{0.05}$/pD fully saturated with Zn^{2+} or Mn^{2+} resulted in better stretching than $pA_{0.05}$/pD without M^{2+}. However, this trend was not immediately obtained from tensile testing. Fibers were prepared from pA/pD and $pA_{0.05}$/pD-M^{2+} coacervates with 0.05 M NaCl and left to dry for 2 days. After drying the fibers were very brittle. The tensile results within the same batch varied largely due to the the brittleness of the dried material. Table 10 and Figure 12 compare selected runs, for all runs per batch see the Appendix Figures 23 and 24. pA/pD shows the biggest elongation of 10.00%, which also gives it the highest toughness of 0.0019 Pa. Due to the brittleness of the fibers, samples would often break upon loading, which makes the results less reliable.

Table 10: Tensile test data for complex coacervate fibers that were dried overnight. Due to their brittleness the fibers give unreliable results

complex	Metal	young's modulus (Pa)	max strain	max stress (Pa)	toughness (Pa)
pA/pD	-	0.41	10.00%	0.033	0.0019
	-	1.11	3.00%	0.034	0.0005
$pA_{0.05}$/pD	Zn^{2+}	0.76	3.33%	0.022	0.0004
	Mn^{2+}	0.77	6.34%	0.040	0.0015

Table 11: Selected tensile test data for wet complex coacervate fibers.

complex	Metal	Young's modulus (Pa)	strain at break	stress at break (Pa)	toughness (Pa)
	-	0.036	30%	0.0061	0.0018
$pA_{0.05}$/pD	Zn^{2+}	0.090	35%	0.0047	0.0020
	Mn^{2+}	0.220	24%	0.0128	0.0035

3.5.2 Wet fibers

To decrease the brittle properties, fiber properties were immediately measured after spinning, see Figure 13. These 'wet' fibers showed an increased strain at break, stress at break, and toughness than their 'dry' counterparts, as seen in the data of Table 11. For the full data see Table 12 in the appendix.
Due to the overall increased toughness, the difference between the coacervate fibers is now noticable in the stress strain curves. Unfortunately, the fibers prepared with $pA_{0.05}$/pD without metal still would often break upon loading. On the contrary, $pA_{0.05}$/pD-Zn^{2+} shows a consistent increased strain and toughness of the fibers. $pA_{0.05}$/pD-Mn^{2+} also shows several samples with increased toughness, but less consistent than $pA_{0.05}$/pD-Zn^{2+} fibers.

Figure 11: Vertical setup of syringe pump that is in direct contact with the coagulation bath. The coagulation bath can consist of water, ethanol or a micture of both.

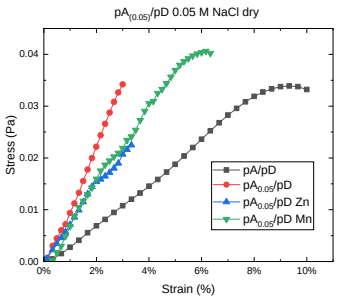

Figure 12: tensile tests of pA/pD and $pA_{0.05}$/pD(M^{2+}) fibers after drying overnight

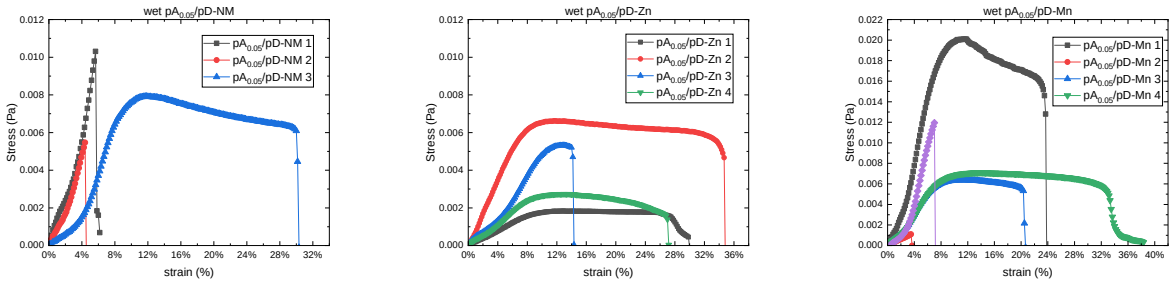

(a) **(b)** **(c)**

Figure 13: tensile tests with multiple runs of wet fibers made with coacervate systems **(a)** $pA_{0.05}$/pD-NM, (b) $pA_{0.05}$/pD-Zn^{2+}, **(c)** $pA_{0.05}$/pD-Mn^{2+} .

3.6 Alignment of polymeric chains

The goal of this project was to create permanently aligning the polymer chains by transiently crosslinking the polyelectrolytes in complex coacervates. Up to now we have seen that the tensile strength increases for the crosslinked fibers, but we do not know if this is also paired with an increase of anisotropy. Therefore, Polarized Optical Microscopy (POM) and Wide-Angle X-ray Scattering (WAXS) were used to characterize the alignment of polymeric chains.

3.6.1 Polarized optical microscopy (POM)

Polarized light microscopy was employed to characterize anisotropy for selected fiber systems. the $pA_{0.05}$/pD complexes were used to prepare the fibers with Zn^{2+}, Mn^{2+} or without metal. After production the fibers were strained by 10% to enforce alignment of the polymeric chains. The POM images in Figure 14 all show the fibers having a pink color, indicating isotropy. Even the strained and crosslinked fibers of $pA_{0.05}$/pD-Zn^{2+} and $pA_{0.05}$/pD-Mn^{2+} exhibit the same color as non strained $pA_{0.05}$/pD fibers which do not contain crosslinks due to the absence metals.

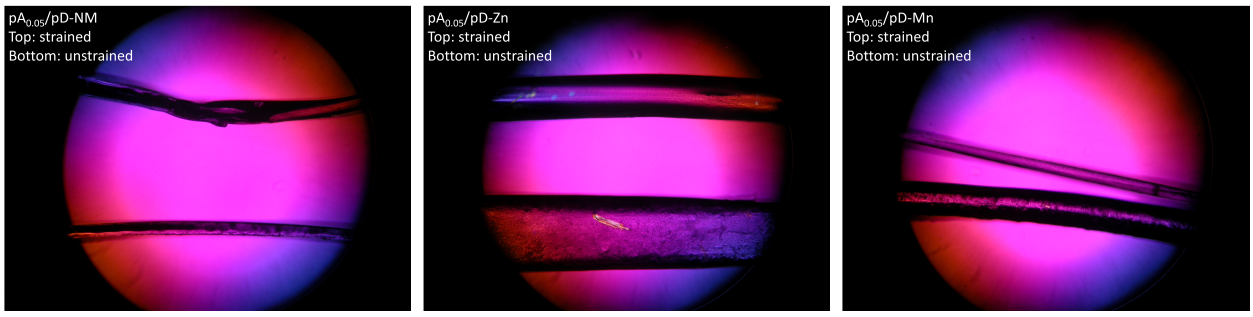

(a) **(b)** **(c)**

Figure 14: POM images of **(a)** pA0.05-NM, **(b)** pA0.05-Zn^{2+}, and **(c)** pA0.05-Mn^{2+}

3.6.2 Wide Angle X-ray Scattering (WAXS)

In addition to POM, alignment of polymeric chains on nm scale was also characterized by Wide-Angle X-ray Scattering (WAXS) for selected produced fibers and strained variants. WAXS diagrams in

Figure 15a show a similar response for all samples. The broad scattering band is typical for amorphous structures. All the diagrams show a scattering maximum at 15 nm^{-1}, corresponding to 0.42 nm. This distance is usually considered to arise from Van Der Waal spacing between non bonded atoms [13]. All prepared samples have the same maximum scattering, meaning that the structure does change after incorporation of Tpy crosslinks. The difference in overall intensity between the samples is explained by the inconsistent fiber thickness, since thicker fibers create a larger overall intensity.
The normalized Q-space intensity diagram in Figure 15b shows an increased intensity at the right hand of the maximum for the $pA_{0.05}$/pD-Mn^{2+} samples. This is true for both the non strained and strained fibers. Also $pA_{0.05}$/pD-Zn^{2+} shows a slight increase in the area of 16 nm^{-1} and 23 nm^{-1}. This trend can be explained by the presence of metals in these fibers, thus creating crosslinks with Tpy units. By forming the crosslinks the Tpy units are closer to each other and thus create a pattern that can be seen in WAXS. In addition, the presence of metals increase the electron density, thus increasing the overall intensity.
Figure 15c depicts the relative azimuthal integration of the scattering intensity. See Figure 27 in the appendix for the raw azimuthal intensity and individual data. All samples show a clear periodic change based on the azimuthal angle, indicating a presence of orientation. A minimum scattering intensity is observed at 90°and 270°for all samples, while a maximum intensity is observed at 180°. The maximum intensity being at 180°shows that the orientation is parallel to the length of the fiber. The orientation is seen at both the strained and non-deformed fibers, indicating that the orientation is not increased due to the crosslinks or straining. The observed orientation could be obtained by the extrusion shear forces of the fibers coming out of the syringe. The minimums have a different height due to the sample fibers having inhomogeneity in the thickness within the same sample. At the maximum and minimums sharp downward peaks are observed. These peaks are caused by the setup of the beam stop of the machine.
Another way to analyze the WAXS pattern is by comparing the equatorial and meridional of the pattern. For example, the diagram in Figure 15d shows the patterns for a $pA_{0.05}$/pD-Mn^{2+} fiber. For all measured diagrams (Figures 28 and 29 in the appendix) no clear difference was observed between the equatorial and meridional integration of the WAXS pattern.

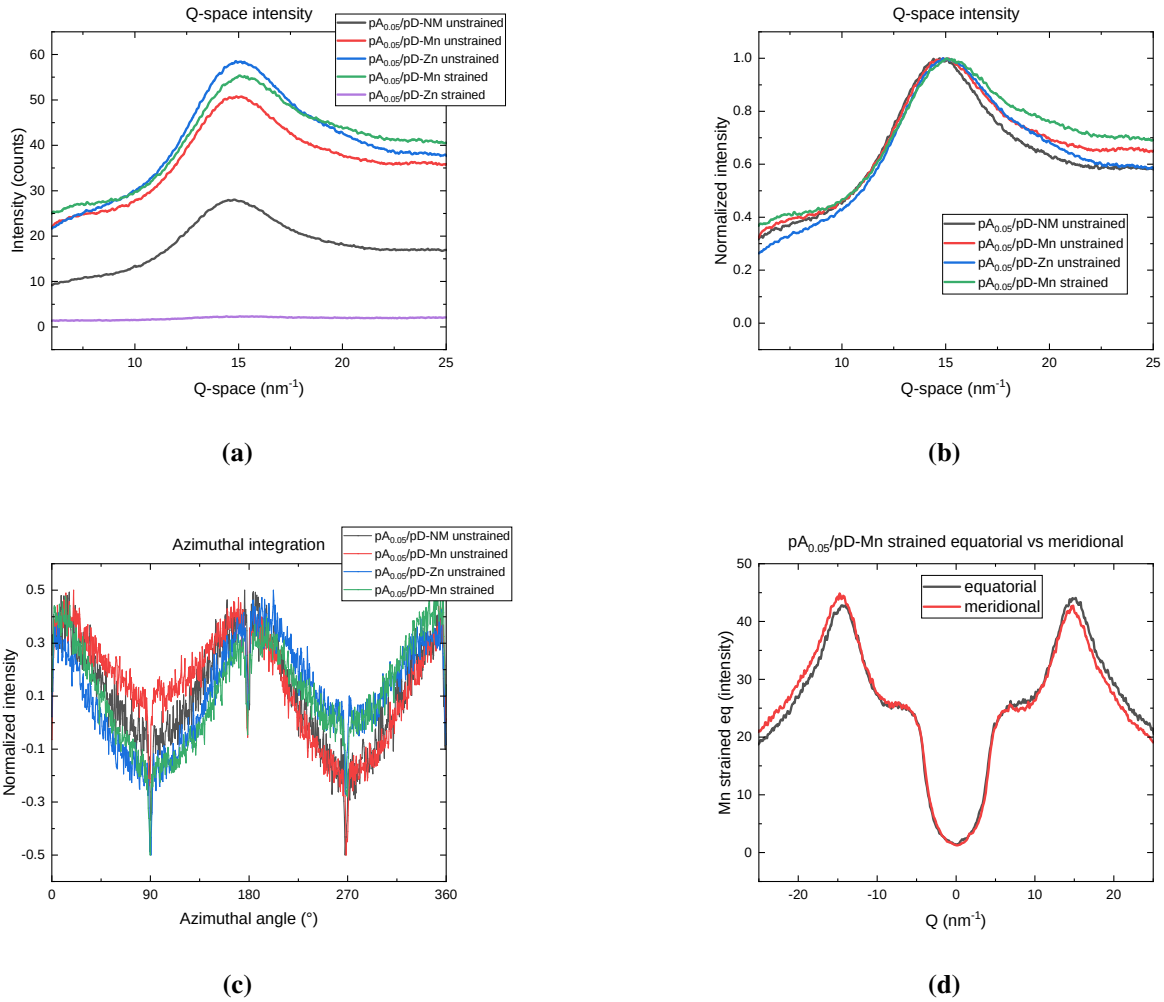

Figure 15: **(a)** WAXS intensity plotted against the Q-value. **(b)** normalized intensity of the count plotted against the Q-value. $pA_{0.05}/pD\text{-}Zn^{2+}$ is not included because its overall weak intensity. **(c)** Orientation intensity diagrams from WAXS data. **(d)** Equatorial and meridional intensity of strained $pA_{0.05}/pD\text{-}Mn$ fiber.

4 Conclusion and Outlook

In this report I demonstrate toughening of complex coacervates by incorporation of Tpy crosslinkers. While an increased tensile strength is seen for the crosslinked complex coacervate fibers, an increased alignment of polymer chains is not observed.

We have seen that the physical properties of complex coacervates can be modified using several parameters. For one, the properties depend on which polyelectrolyte the Tpy units are attached. Crosslinking the $pA_{0.05}$/pD complexes results in an increased viscosity and maximum stretching. On the contrary, crosslinks on the pA/$pD_{0.05}$ systems result in a gel that cannot be stretched, unless the metal concentration is reduced to a minimum and the NaCl concentration is increased significantly. Just like the pA/$pD_{0.05}$ system, complexes with terpyridine on both polyelectrolytes ($pA_{0.05}$/$pD_{0.05}$) become a non-stretchable gel upon addition of metals. This observed dependence of on which polyelectrolyte Tpy is grafted can be explained by the molecular weight of the polymers. The used pD had a much larger molecular weight than pA. Because of the longer polymer chains of pD, entanglements of the chains are more likely upon crosslinking. This theory can be verified by preparing crosslinked $pA_{0.05}$/pD complex coacervates with a high molecular weight pA and low weight pD.

Another parameter for changing the properties is the number of Tpy units that are grafted on the polyelectrolyte. As expected, the less grafted $pA_{0.025}$/pD complexes show a lower viscosity and work of adhesion than the $pA_{0.05}$/pD systems, because there are less crosslinks in the lower grafted system. Higher grafting was not tested, but increasing the grafting to create $pA_{0.1}$/pD should enhance the viscosity, work of adhesion, and toughness even more.
In addition, different divalent metals can be used for crosslinking to achieve distinct responses. We have seen a recurring order in which the metals increase the viscosity and work of adhesion. This order also agrees with the order of binding affinity found in literature [8]. Interestingly, Co^{2+} is supposed to have a high binding affinity with terpyridine, but this trend is not seen in the recorded data. Thus a higher binding affinity of the metal does not necessarily lead to a higher viscosity or work of adhesion of the complex coacervate. This finding highlights the complexity of rheological experiments. Co^{2+} could possibly display its strong binding properties in a rheological experiment that is more relevant to the binding affinity.

The effect of exceeding the 2:1 ratio of Tpy:M^{2+} in coacervates is also explored. We found that for $pA_{0.05}$/pD coacervates a longer maximum stretching is observed when using a 2:2 ratio of Tpy:M^{2+}, compared to the normally used 2:1 ratio. However, oscillation frequency sweeps do not show a clear difference of storage and loss moduli between coacervates with the ratios. This difference in the findings can be explained by the larger deformation caused during the stretching experiments. A rheological experimental method that mimics the large shear of stretching could show a distinct effect of exceeding the 2:1 ratio of Tpy:M^{2+}.

Fibers are best produced by vertically injecting them into a coagulation bath with ethanol. After overnight drying the fibers become very brittle and the effect of crosslinking is no longer observed in tensile testing. When tensile testing is performed while the fibers are still wet, the effect of crosslinking is observed as an increase in toughness. One of the recurring problems for the production of the tensile testing was that the fibers being too brittle for accurate testing. The system can be toughened by using higher molecular weight variants of the polyelectrolytes. But, increasing the molecular weight might cause difficulties in water solubility of the polymers. Therefore, it is certainly worth

looking into a new polyelectrolyte system. If the new system also has a high critical salt concentration, R.O. water can be used as the coagulation bath when producing fibers.

WAXS measurements of the prepared fibers show the pattern distance between Tpy groups when metals are included in the coacervate fibers. Orientation in the length of the fiber is observed by azimuthal integration of the WAXS pattern, regardless of straining and the presence of metals in the sample. The observed orientation could be arising from the extrusion processing of the fibers. Coacervate systems with Tpy crosslinks with the used metals unfortunately do not show substantial alignment of the polymer chains. Using a divalent metal with a higher binding affinity can create stronger crosslinking, and in turn enforce alignment.

Currently, it is assumed that after stretching the fibers alignment is obtained, but is lost due to relaxation. A WAXS analysis of the fibers while strained in the setup could prove this theorized alignment before relaxation.

Bibliography

[1] C. H. Porcel and J. B. Schlenoff, "Compact polyelectrolyte complexes: "saloplastic" candidates for biomaterials," *Biomacromolecules*, vol. 10, no. 11, pp. 2968–2975, 2009. PMID: 19835412.

[2] A. S. Michaels, "Polyelectrolyte complexes," *Industrial & Engineering Chemistry*, vol. 57, no. 10, pp. 32–40, 1965.

[3] J. van der Gucht, E. Spruijt, M. Lemmers, and M. A. Cohen Stuart, "Polyelectrolyte complexes: Bulk phases and colloidal systems," *Journal of Colloid and Interface Science*, vol. 361, no. 2, pp. 407–422, 2011.

[4] J. Sun, *Unpublished results*. 2021.

[5] Y. Termonia, "Molecular modeling of spider silk elasticity," *Macromolecules*, vol. 27, no. 25, pp. 7378–7381, 1994.

[6] M. L. Tanzer, "Cross-linking of collagen," *Science*, vol. 180, no. 4086, pp. 561–566, 1973.

[7] L. M. Dowling, W. G. Crewther, and A. S. Inglis, "The primary structure of component 8c-1, a subunit protein of intermediate filaments in wool keratin. Relationships with proteins from other intermediate filaments," *Biochemical Journal*, vol. 236, pp. 695–703, 06 1986.

[8] A. D. Filippov, J. Sprakel, and M. Kamperman, "Complex coacervation and metal–ligand bonding as synergistic design elements for aqueous viscoelastic materials," *Soft Matter*, vol. 17, pp. 3294–3305, 2021.

[9] I. Henderson, "Tuning the properties of metal-ligand complexes to modify the properties of supramolecular materials," 11 2021.

[10] D. R. Burfield and R. H. Smithers, "Desiccant efficiency in solvent drying. 3. dipolar aprotic solvents more about this article," *J. Org. Chem*, pp. 3966–3968, 1978.

[11] M. Dompé, F. J. Cedano-Serrano, O. Heckert, N. van den Heuvel, J. van der Gucht, Y. Tran, D. Hourdet, C. Creton, and M. Kamperman, "Thermoresponsive complex coacervate-based underwater adhesive," *Advanced materials (Deerfield Beach, Fla.)*, vol. 31, p. e1808179, May 2019.

[12] R. Dobrawa, P. Ballester, C. R. Saha-Möller, and F. Würthner, *Thermodynamics of 2,2':6',2"-Terpyridine-Metal Ion Complexation*, ch. 4, pp. 43–62.

[13] R. L. Miller, R. F. Boyer, and J. Heijboer, "X-ray scattering from amorphous acrylate and methacrylate polymers: Evidence of local order," *Journal of Polymer Science: Polymer Physics Edition*, vol. 22, no. 12, pp. 2021–2041, 1984.

Appendices

A NMR

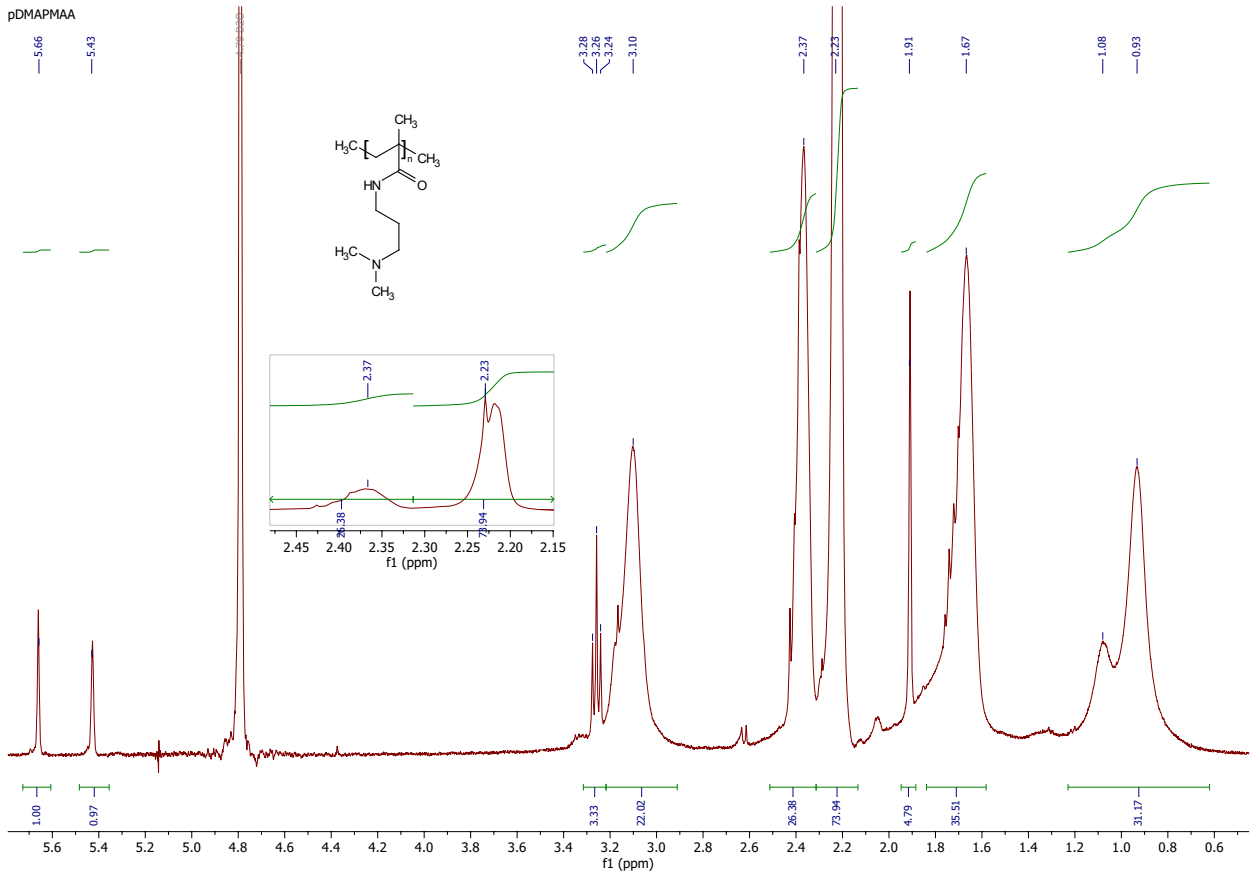

Figure 16: Proton NMR spectrum of pDMAPMAA (400 MHz, D_2O).

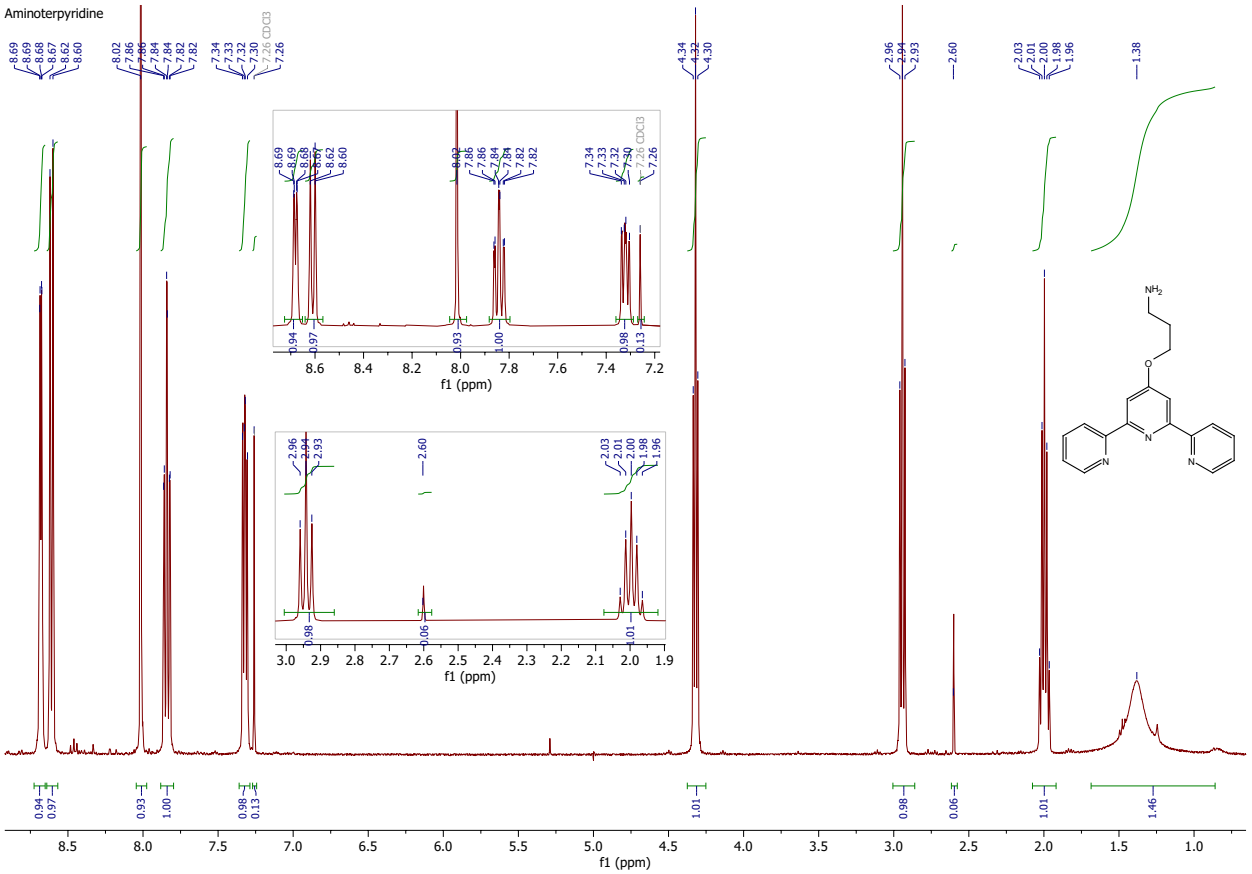

Figure 17: Proton NMR spectrum of aminoterpyrdine (400 MHz, $CDCl_3$).

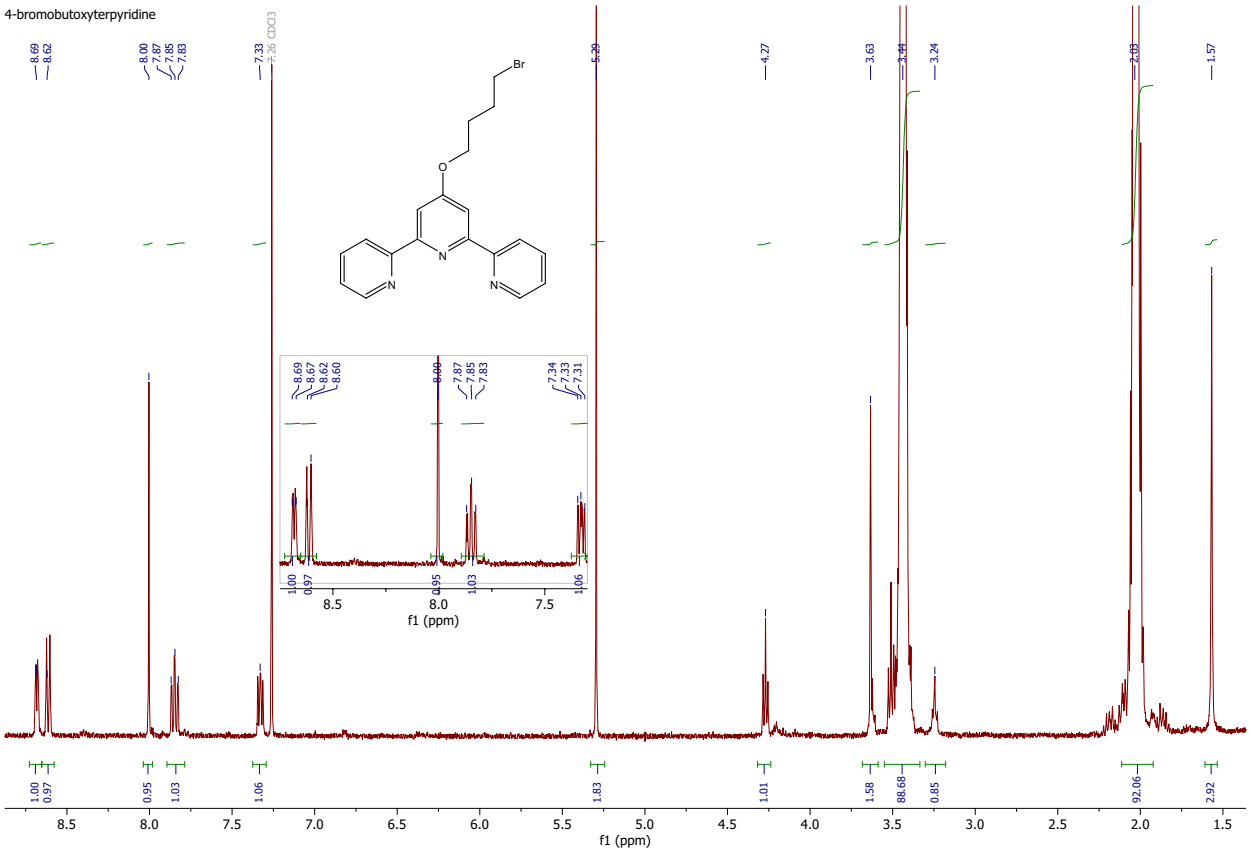

Figure 18: Proton NMR spectrum of bromoterpyridine (400 MHz, $CDCl_3$).

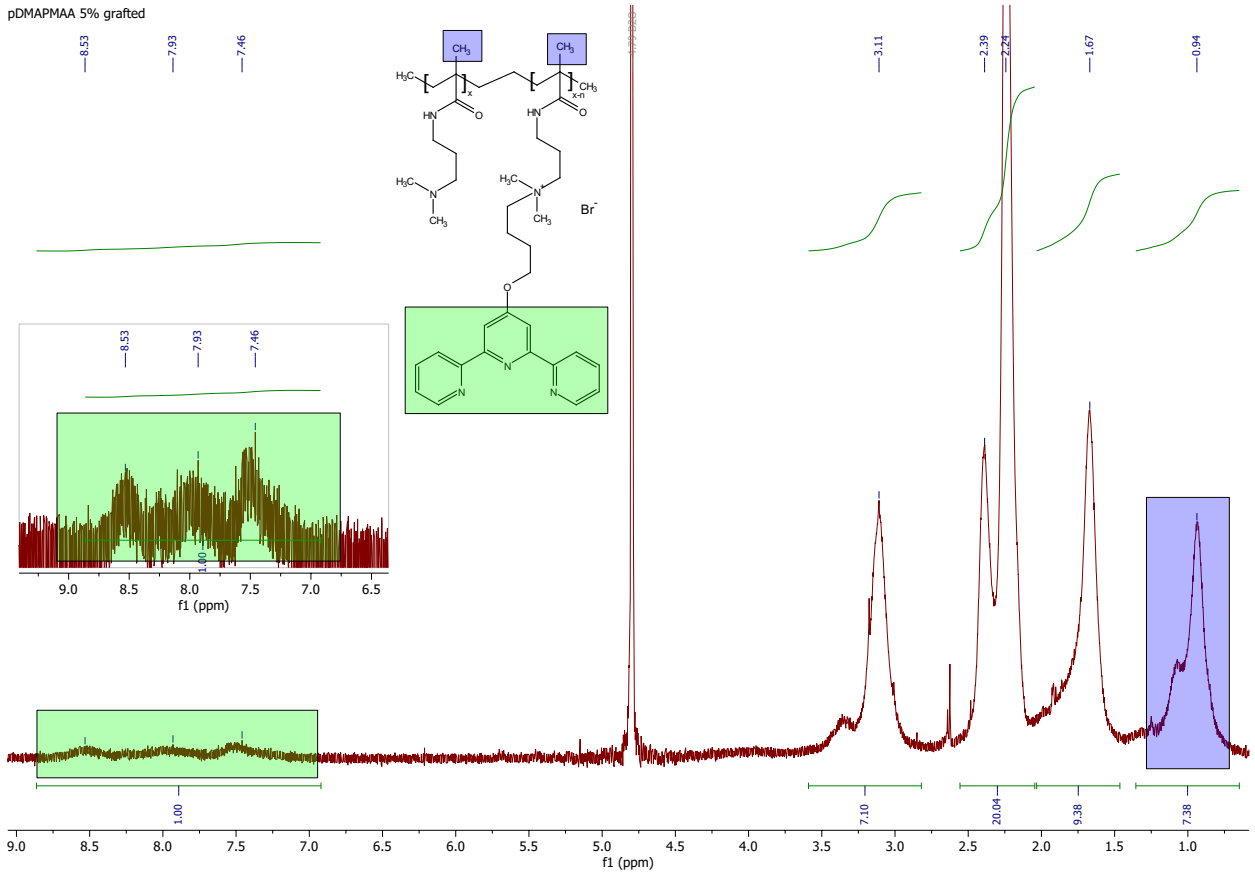

Figure 19: Proton NMR spectrum of 5% terpyrilated pDMAPMAA (400 MHz, D_2O). Analysis of the integrals of the colored regions shows an actual grafting percentage of 3.8%

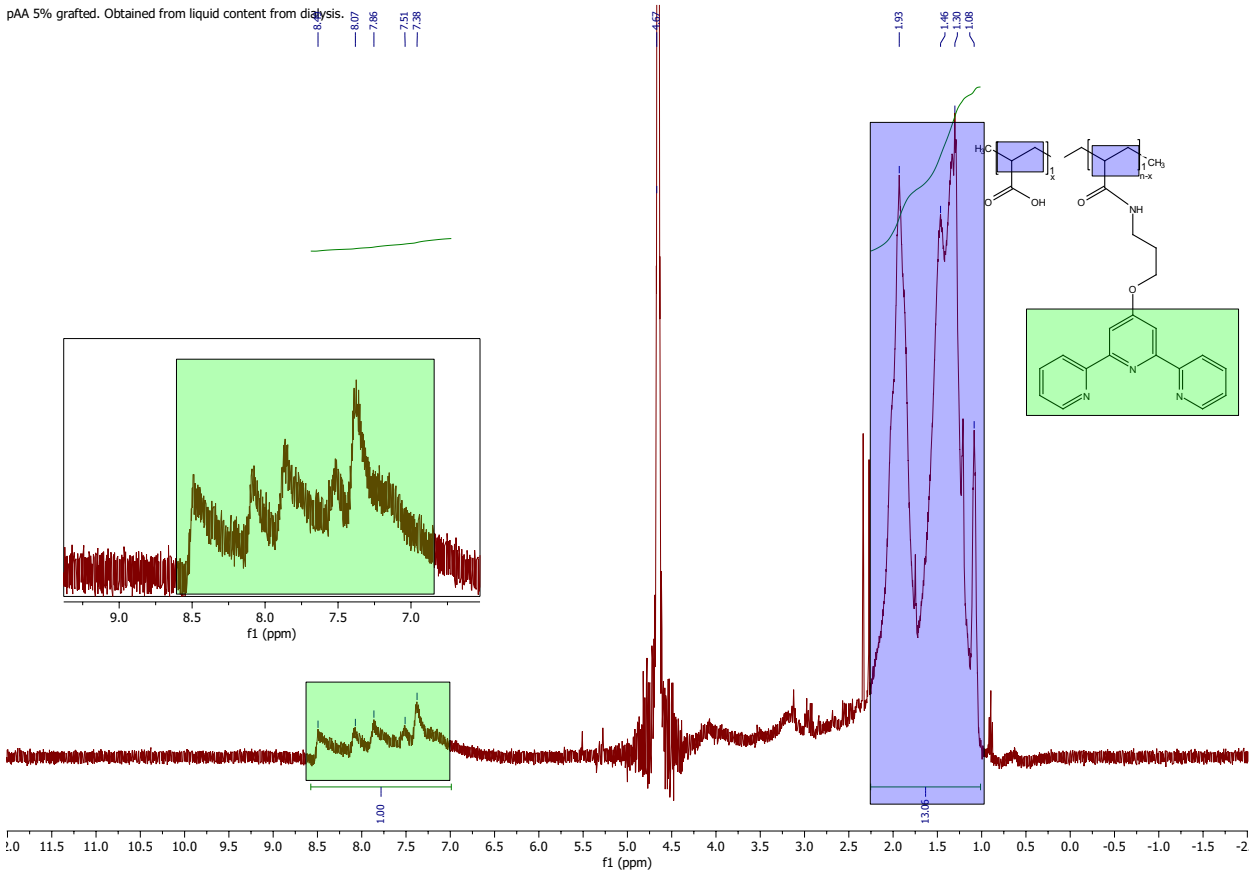

Figure 20: Proton NMR spectrum of 5% terpyrilated pAA obtained from the liquid content from the dialysis (400 MHz, D_2O). Analysis of the integrals of the colored regions shows an actual grafting percentage of 2.3%

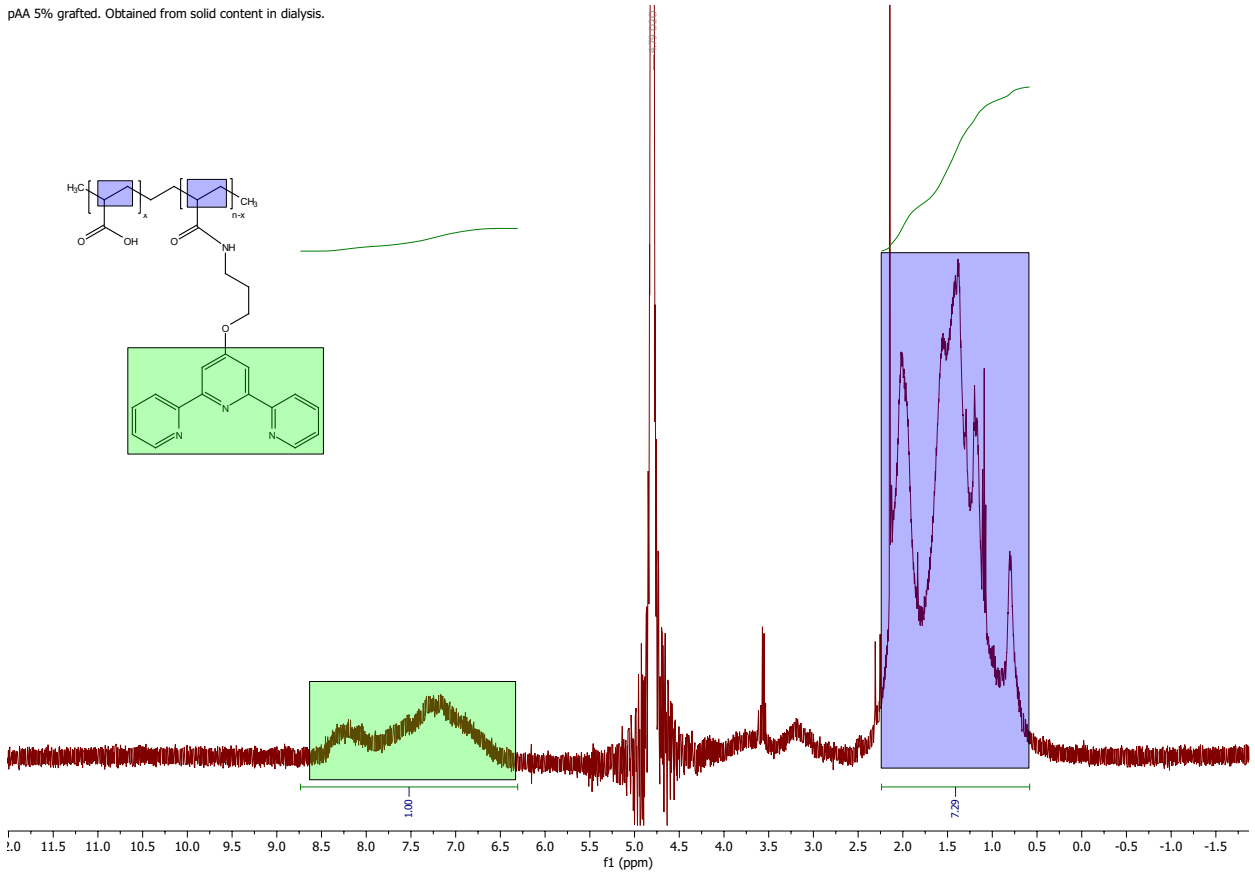

Figure 21: Proton NMR spectrum of 5% terpyrilated pAA obtained from the solid content from the dialysis (400 MHz, D_2O). Analysis of the integrals of the colored regions shows an actual grafting percentage of 4.1%

B Rheology

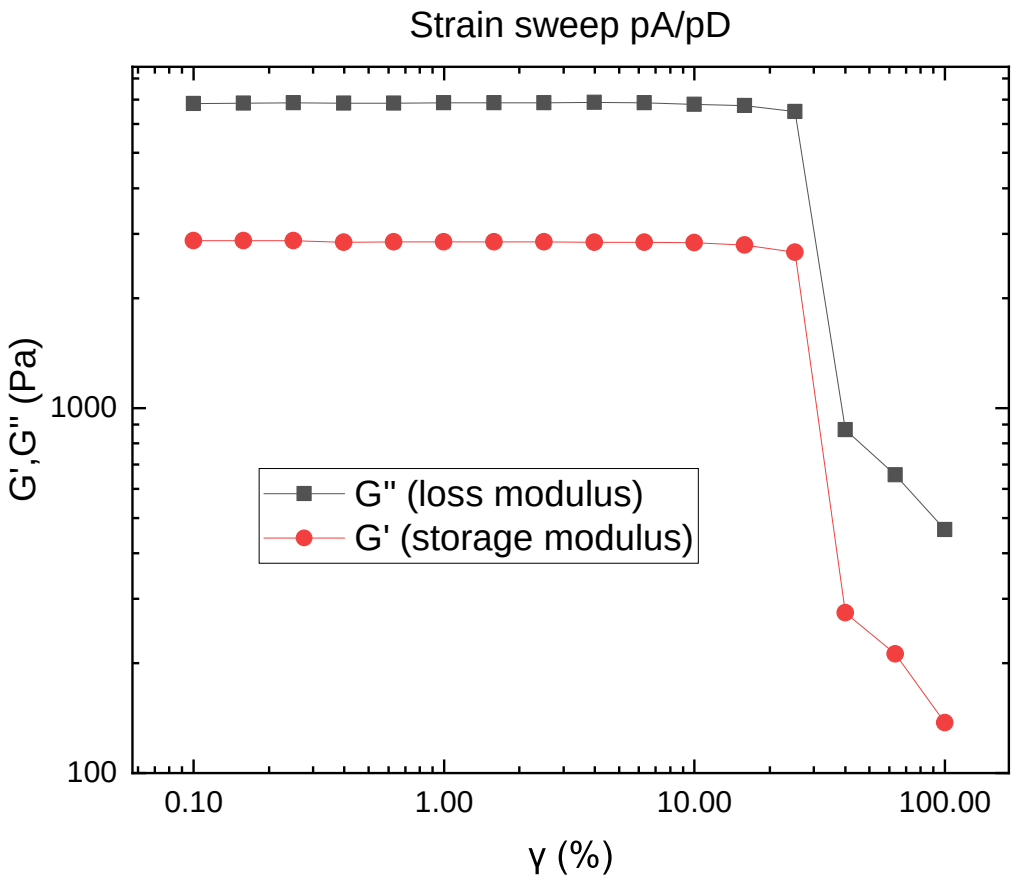

Figure 22: Strain sweep storage (G') and loss (G") moduli of pA/pD.

C Tensile test data

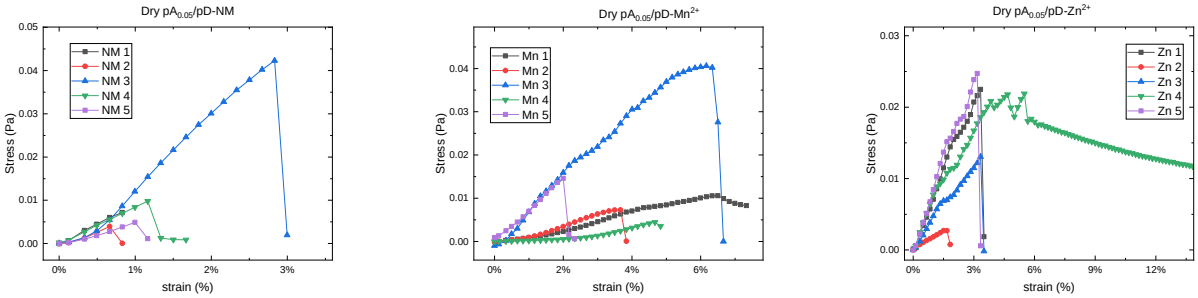

(a) **(b)** **(c)**

Figure 23: Tensile test stress strain curves for dry fibers **(a)** $pA_{0.05}$/pD-NM **(b)** $pA_{0.05}$/pD-Mn^{2+} and **(c)** $pA_{0.05}$/pD-Zn^{2+}

.

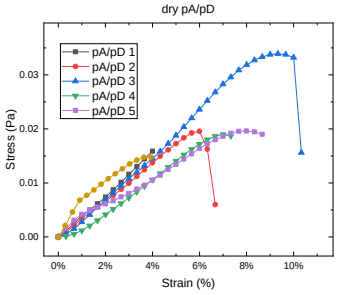

Figure 24: tensile test stress strain curve pA/pD

Table 12: Tensile testing data for stress strain curves of wet fibers in Figure 13.

system	sample	young's modulus (Pa)	strain at break	maximum stress (Pa)	toughness (Pa)
$pA_{0.05}$/pD-NM	1	0.131	5.7%	0.0103	0.0002
	2	0.075	4.4%	0.0055	0.0001
	3	0.036	30.0%	0.0073	0.0018
	average NM	0.080	13.4%	0.0077	0.0007
$pA_{0.05}$/pD-Mn^{2+}	1	0.220	23.7%	0.0200	0.0035
	2	0.031	3.5%	0.0011	0.0000
	3	0.058	20.3%	0.0064	0.0011
	4	0.056	38.3%	0.0071	0.0020
	5	0.047	7.0%	0.0119	0.0003
	average Mn^{2+}	0.082	18.6%	0.0093	0.0014
$pA_{0.05}$/pD-Zn^{2+}	1	0.019	29.8%	0.0018	0.0005
	2	0.090	34.7%	0.0066	0.0021
	3	0.031	14.2%	0.0053	0.0004
	4	0.025	27.0%	0.0027	0.0005
	average Zn^{2+}	0.041	26.4%	0.0041	0.0009

D WAXS imaging

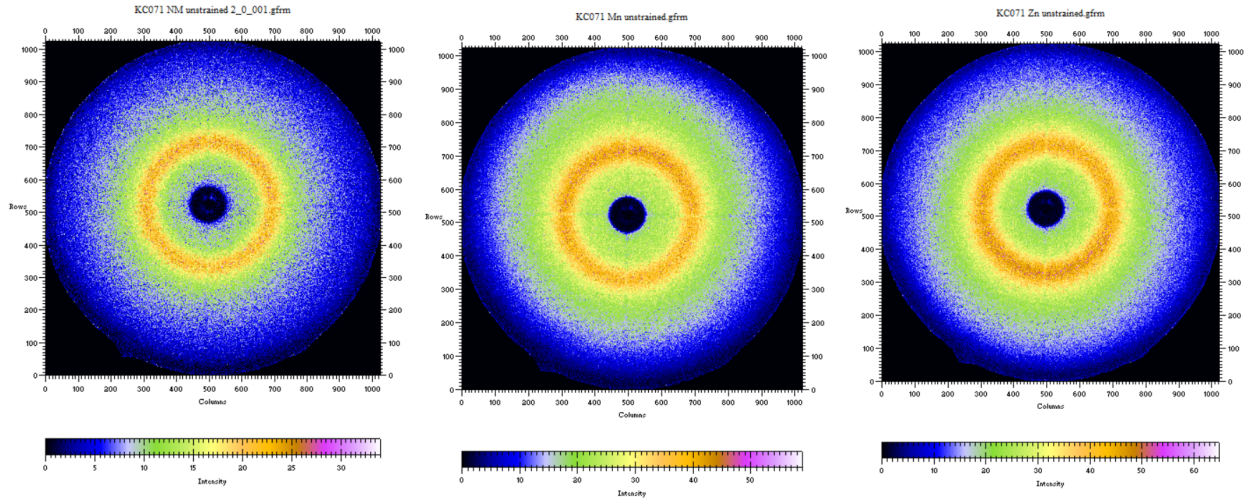

(a) **(b)** **(c)**

Figure 25: WAXS patterns of non strained **(a)** $pA_{0.05}$/pD with no metal, **(b)** $pA_{0.05}$/pD-Mn^{2+}, and **(c)** $pA_{0.05}$/pD-Zn^{2+} fibers

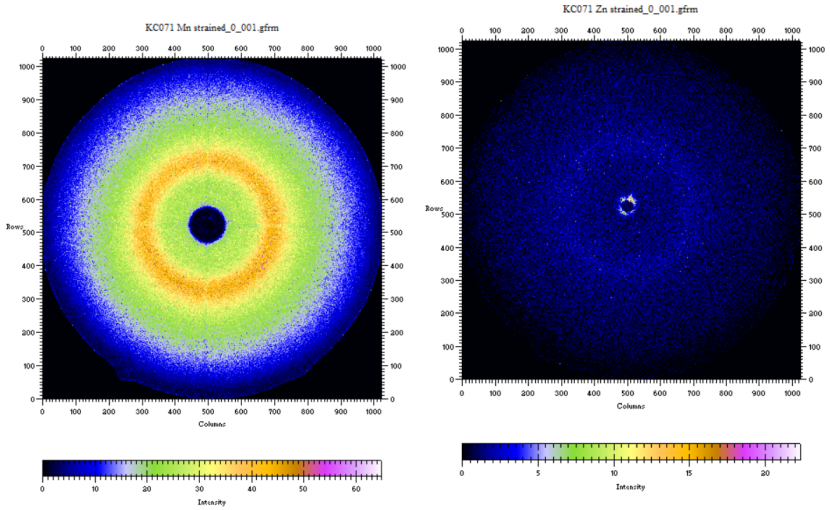

(a) **(b)**

Figure 26: WAXS patterns of 10% strained **(a)** $pA_{0.05}$/pD-Mn^{2+}, **(b)**$pA_{0.05}$/pD-Zn^{2+} fibers. Note that the intensity is very weak for $pA_{0.05}$/pD-Zn^{2+} due to the fiber being very thin.

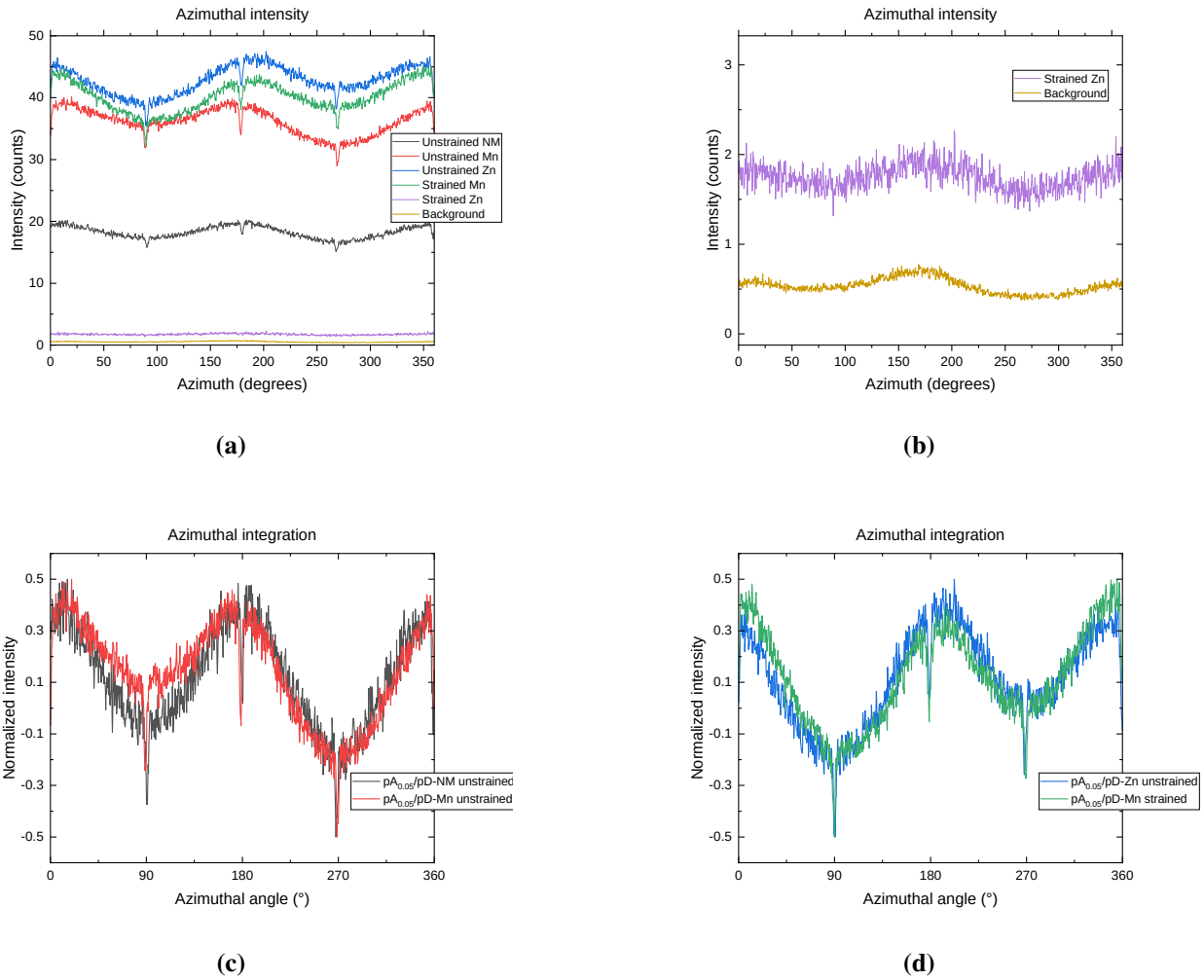

Figure 27: Azimuthal integration **(a)** The raw azimuthal integration data **(b)** The azimuthal integration zoomed in **(c)** The relative azimuthal integration of unstrained $pA_{0.05}$/pD-NM and $pA_{0.05}$/pD-Mn fibers. **(d)** The relative azimuthal integration of unstrained $pA_{0.05}$/pD-Zn and strained $pA_{0.05}$/pD-Mn fibers.

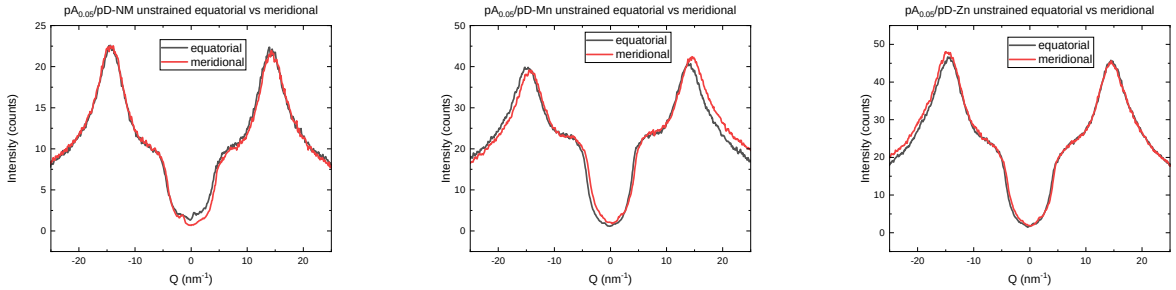

(a) **(b)** **(c)**

Figure 28: equatorial and meridonial integration of the WAXS patterns of non strained **(a)** $pA_{0.05}$/pD with no metal, **(b)** $pA_{0.05}$/pD-Mn^{2+}, and **(c)** $pA_{0.05}$/pD-Zn^{2+} fibers

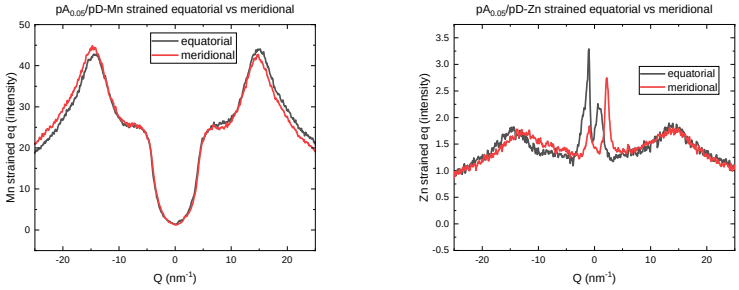

(a) **(b)**

Figure 29: equatorial and meridonial integration of the WAXS patterns of 10% strained **(a)** $pA_{0.05}$/pD-Mn^{2+}, **(b)** $pA_{0.05}$/pD-Zn^{2+} fibers. Note that the intensity is very weak for $pA_{0.05}$/pD-Zn^{2+} due to the fiber being very thin.